

# [Ir(COD)Cl]<sub>2</sub> as a Catalyst Precursor for the Intramolecular Hydroamination of Unactivated Alkenes with Primary Amines and Secondary Alkyl- or Arylamines: A Combined Catalytic, Mechanistic, and Computational Investigation

Kevin D. Hesp,<sup>†</sup> Sven Tobisch,<sup>\*,‡</sup> and Mark Stradiotto<sup>\*,†</sup>

Department of Chemistry, Dalhousie University, Halifax, Nova Scotia B3H 4J3, Canada, and  
School of Chemistry, University of St Andrews, St Andrews, KY16 9ST, United Kingdom

Received September 30, 2009; E-mail: mark.stradiotto@dal.ca; st40@st-andrews.ac.uk

**Abstract:** The successful application of [Ir(COD)Cl]<sub>2</sub> as a precatalyst for the intramolecular addition of primary as well as secondary alkyl- or arylamines to unactivated olefins at relatively low catalyst loading is reported (25 examples), along with a comprehensive experimental and computational investigation of the reaction mechanism. Catalyst optimization studies examining the cyclization of *N*-benzyl-2,2-diphenylpent-4-en-1-amine (**1a**) to the corresponding pyrrolidine (**2a**) revealed that for reactions conducted at 110 °C neither the addition of salts (N<sup>+</sup>Bu<sub>4</sub>Cl, LiOTf, AgBF<sub>4</sub>, or LiB(C<sub>6</sub>F<sub>5</sub>)<sub>4</sub>·2.5OEt<sub>2</sub>) nor phosphine coligands served to enhance the catalytic performance of [Ir(COD)Cl]<sub>2</sub>. In this regard, the rate of intramolecular hydroamination of **1a** employing [Ir(COD)Cl]<sub>2</sub>/L<sub>2</sub> (L<sub>2</sub> = 2-(di-*t*-butylphosphino)biphenyl) catalyst mixtures exhibited an inverse-order dependence on L<sub>2</sub> at 65 °C, and a zero-order rate dependence on L<sub>2</sub> at 110 °C. However, the use of 5 mol % HNEt<sub>3</sub>Cl as a cocatalyst was required to promote the cyclization of primary aminoalkene substrates. Kinetic analysis of the hydroamination of **1a** revealed that the reaction rate displays first order dependence on the concentration of Ir and inverse order dependence with respect to both substrate (**1a**) and product (**2a**) concentrations; a primary kinetic isotope effect (*k*<sub>H</sub>/*k*<sub>D</sub> = 3.4(3)) was also observed. Eyring and Arrhenius analyses for the cyclization of **1a** to **2a** afforded Δ*H*<sup>‡</sup> = 20.9(3) kcal mol<sup>−1</sup>, Δ*S*<sup>‡</sup> = −23.1(8) cal/K·mol, and *E*<sub>a</sub> = 21.6(3) kcal mol<sup>−1</sup>, while a Hammett study of related arylaminoalkene substrates revealed that increased electron density at nitrogen encourages hydroamination (ρ = −2.4). Plausible mechanisms involving either activation of the olefin or the amine functionality have been scrutinized computationally. An energetically demanding oxidative addition of the amine N–H bond to the Ir<sup>I</sup> center precludes the latter mechanism and instead activation of the olefin C=C bond prevails, with [Ir(COD)-Cl(substrate)] **M1** representing the catalytically competent compound. Notably, such an olefin activation mechanism had not previously been documented for Ir-catalyzed alkene hydroamination. The operative mechanistic scenario involves: (1) smooth and reversible nucleophilic attack of the amine unit on the metal-coordinated C=C double bond to afford a zwitterionic intermediate; (2) Ir–C bond protonolysis via stepwise proton transfer from the ammonium unit to the metal and ensuing reductive elimination; and (3) final irreversible regeneration of **M1** through associative cycloamine expulsion by new substrate. DFT unveils that reductive elimination involving a highly reactive and thus difficult to observe Ir<sup>III</sup>-hydrido intermediate, and passing through a highly organized transition state structure, is turnover limiting. The assessed effective barrier for cyclohydroamination of a prototypical secondary alkylamine agrees well with empirically determined Eyring parameters.

## Introduction

The hydroamination of alkenes, alkynes, and related unsaturated substrates represents an attractive strategy for the construction of nitrogen-containing compounds that circumvents the formation of byproduct in the creation of a C–N linkage.<sup>1</sup> In particular, intramolecular variants of these reactions are appealing as atom-economical routes to nitrogen-containing heterocycles that are prevalent in naturally occurring and/or biologically active molecules.<sup>2</sup> Although the synthetic potential of cyclohydroamination is significant, general methods for promot-

ing the intramolecular hydroamination of unactivated aminoalkenes under mild conditions and with broad substrate scope are still lacking. A diverse number of catalyst systems are known to effect such cyclizations,<sup>1a</sup> including (but not restricted to) those based on rare earth elements and actinides,<sup>3</sup> alkali and alkaline earth metals,<sup>4</sup> Group 4 metals,<sup>5</sup> and Brønsted acids;<sup>6</sup> nonetheless, the pursuit of increased substrate scope and functional group tolerance has prompted the development of alternative catalysts based on metals from Groups 8–11. While progress has been made in the use of Fe,<sup>7</sup> Pd,<sup>8</sup> and Au<sup>9,10</sup> catalysts for the intramolecular addition of secondary amides, carbamates, or ureas to unactivated olefins, the identification of late metal catalysts for analogous transformations involving

<sup>†</sup> Dalhousie University.<sup>‡</sup> University of St Andrews.

secondary alkyl- or arylamines, as well as primary amines, has proven more elusive. The first catalyst system of this type was described in 2005 by Widenhoefer and co-workers,<sup>11</sup> who reported the use of  $[\text{PtCl}_2(\text{H}_2\text{C}=\text{CH}_2)]_2/\text{PPH}_3$ <sup>11a</sup> and later  $\text{PtCl}_2/$

biarylphosphine<sup>11b</sup> for the cyclization of secondary alkylaminoalkenes, including one example involving a 1,1-disubstituted olefin. In 2008, Liu and Hartwig<sup>12</sup> disclosed the use of  $[\text{Rh}(\text{COD})_2]\text{BF}_4/\text{Cy-DavePhos}$  ( $\text{COD} = \eta^4\text{-cyclooctadiene}$ ;  $\text{Cy-DavePhos} = 2\text{-dicyclohexylphosphino-2'-}N,N\text{-dimethylamino-biphenyl}$ ) for the hydroamination of aminoalkenes that feature primary or secondary alkylamines and terminal or internal alkenes. In the same year, the use of Rh and Ir complexes supported by pincer-type *N*-heterocyclic carbene ligands for the cyclization of terminal alkenes by pendant secondary alkyl- and phenylamines was described by Hollis and co-workers.<sup>13</sup> Following the appearance of our preliminary report in this area,<sup>14</sup> Sawamura and co-workers<sup>15</sup> disclosed the use of  $\text{Cu}(\text{O}^i\text{Bu})/\text{Xantphos}$  ( $\text{Xantphos} = 4,5\text{-bis(diphenylphosphino)-9,9-dimethylxanthene}$ ) for the hydroamination of alkenes by tethered primary or secondary alkylamines, including an example of a 1,1-disubstituted secondary aminoalkene substrate. Notwithstanding this recent progress, the identification of late metal catalysts for use in promoting the intramolecular addition of primary as well as secondary alkyl- and arylamines to both terminal and internal olefins remains an important and significant challenge. Furthermore, with the exception of the NMR spectroscopic characterization of catalytic intermediates in the breakthrough Pt catalyst system disclosed by Bender and Widenhoefer,<sup>11a</sup> no kinetic or mechanistic data pertaining to the cyclohydroamination of alkylamino-alkenes are provided in the ensuing reports.<sup>12–15</sup>

Encouraged by advances in the Ir-mediated intermolecular hydroamination of activated alkenes,<sup>16–18</sup> as well as recent progress in the Ir-catalyzed cyclohydroamination of alkynes,<sup>16,19</sup> we sought to expand further the synthetic repertoire of late metal-mediated hydroamination through the identification of simple Ir precatalysts that exhibit useful substrate scope in the

- (1) (a) Müller, T. E.; Hultzs, K. C.; Yus, M.; Foubelo, F.; Tada, M. *Chem. Rev.* **2008**, *108*, 3795. (b) Hartwig, J. F. *Nature* **2008**, *455*, 314. (c) Widenhoefer, R. A. *Chem.—Eur. J.* **2008**, *14*, 5382. (d) Chianese, A. R.; Lee, S. J.; Gagné, M. R. *Angew. Chem., Int. Ed.* **2007**, *46*, 4042. (e) Severin, R.; Doye, S. *Chem. Soc. Rev.* **2007**, *36*, 1407. (f) Brunet, J.-J.; Chu, N.-C.; Rodríguez-Zubiri, M. *Eur. J. Inorg. Chem.* **2007**, 4711. (g) Aillaud, I.; Collin, J.; Hannedouche, J.; Schulz, E. *Dalton Trans.* **2007**, 5105. (h) Widenhoefer, R. A.; Han, X. *Eur. J. Org. Chem.* **2006**, 4555. (i) Hultzs, K. C. *Adv. Synth. Catal.* **2005**, *347*, 367. (j) Hultzs, K. C. *Org. Biomol. Chem.* **2005**, *3*, 1819. (k) Alonso, F.; Beletskaya, I. P.; Yus, M. *Chem. Rev.* **2004**, *104*, 3079. (l) Hartwig, J. F. *Pure Appl. Chem.* **2004**, *76*, 507. (m) Roesky, P. W.; Müller, T. E. *Angew. Chem., Int. Ed.* **2003**, *42*, 2708. (n) Pohlki, F.; Doye, S. *Chem. Soc. Rev.* **2003**, *32*, 104. (o) Nobis, M.; Drießen-Hölscher, B. *Angew. Chem., Int. Ed.* **2001**, *40*, 3983. (p) Müller, T. E.; Beller, M. *Chem. Rev.* **1998**, *98*, 675.
- (2) (a) Hong, S.; Kawaoka, A. M.; Marks, T. J. *J. Am. Chem. Soc.* **2003**, *125*, 15878. (b) Trost, B. M.; Tang, W. J. *Am. Chem. Soc.* **2003**, *125*, 8744. (c) Molander, G. A.; Dowdy, E. D.; Pack, S. K. *J. Org. Chem.* **2001**, *66*, 4344. (d) O'Hagan, D. *Nat. Prod. Rep.* **2000**, *17*, 435. (e) Arredondo, V. M.; Tian, S.; McDonald, F. E.; Marks, T. J. *J. Am. Chem. Soc.* **1999**, *121*, 3633.
- (3) For a selection of recent lead references, see: (a) Yuen, H. F.; Marks, T. J. *Organometallics* **2009**, *28*, 2423. (b) Lu, E.; Gan, W.; Chen, Y. *Organometallics* **2009**, *28*, 2318. (c) Aillaud, I.; Collin, J.; Duhayon, C.; Guillot, R.; Lyubov, D.; Schulz, E.; Trifonov, A. *Chem.—Eur. J.* **2008**, *14*, 2189. (d) Ge, S.; Meetsma, A.; Hessen, B. *Organometallics* **2008**, *27*, 5339. (e) Hannedouche, J.; Aillaud, I.; Collin, J.; Schulz, E.; Trifonov, A. *Chem. Commun.* **2008**, 3552. (f) Zi, G.; Xiang, L.; Song, H. *Organometallics* **2008**, *27*, 1242. (g) Stubbart, B. D.; Marks, T. J. *J. Am. Chem. Soc.* **2007**, *129*, 4253. (h) Stubbart, B. D.; Marks, T. J. *J. Am. Chem. Soc.* **2007**, *129*, 6149. (i) Vitanova, D. V.; Hampel, F.; Hultzs, K. C. *J. Organomet. Chem.* **2007**, *692*, 4690. (j) Rastätter, M.; Zulus, A.; Roesky, P. W. *Chem.—Eur. J.* **2007**, *13*, 3606. (k) Riegert, D.; Collin, J.; Daran, J.-C.; Fillebeen, T.; Schulz, E.; Lyubov, D.; Fukin, G.; Trifonov, A. *Eur. J. Inorg. Chem.* **2007**, 1159. (l) Yu, X.; Marks, T. J. *Organometallics* **2007**, *26*, 365. (m) Rastätter, M.; Zulus, A.; Roesky, P. W. *Chem. Commun.* **2006**, 874. (n) Gribkov, D. V.; Hultzs, K. C.; Hampel, F. *J. Am. Chem. Soc.* **2006**, *128*, 3748. (o) Bambirra, S.; Tsurugi, H.; van Leusen, D.; Hessen, B. *Dalton Trans.* **2006**, 1157. (p) Hultzs, K. C.; Gribkov, D. V.; Hampel, F. *J. Organomet. Chem.* **2005**, *690*, 4441. (q) Kim, H.; Lee, H. P.; Livinghouse, T. *Chem. Commun.* **2005**, 5205. (r) Kim, J.-Y.; Livinghouse, T. *Org. Lett.* **2005**, *7*, 4391. (s) Lauterwasser, F.; Hayes, P. G.; Bräse, S.; Piers, W. E.; Schafer, L. L. *Organometallics* **2004**, *23*, 2234. (t) Hong, S.; Marks, T. J. *Acc. Chem. Res.* **2004**, *37*, 673, and references cited therein.
- (4) For some recent references, see: (a) Zhang, W.; Werness, J. B.; Tang, W. *Tetrahedron* **2009**, *65*, 3090. (b) Crimmin, M. R.; Arrowsmith, M.; Barrett, A. G. M.; Casely, I. J.; Hill, M. S.; Procopiou, P. A. *J. Am. Chem. Soc.* **2009**, *131*, 9670. (c) Arrowsmith, M.; Hill, M. S.; Kociok-Köhn, G. *Organometallics* **2009**, *28*, 1730. (d) Datta, S.; Gamer, M. T.; Roesky, P. W. *Organometallics* **2008**, *27*, 1207. (e) Martinez, P. H.; Hultzs, K. C.; Hampel, F. *Chem. Commun.* **2006**, 2221.
- (5) For a selection of recent lead references, see: (a) Lee, A. V.; Sajitz, M.; Schafer, L. L. *Synthesis* **2009**, 97. (b) Lian, B.; Spaniol, T. P.; Horrillo-Martinez, P.; Hultzs, K. C.; Okuda, J. *Eur. J. Inorg. Chem.* **2009**, 429. (c) Cho, J.; Hollis, T. K.; Helgert, T. R.; Valente, E. J. *Chem. Commun.* **2008**, 5001. (d) Xiang, L.; Song, H.; Zi, G. *Eur. J. Inorg. Chem.* **2008**, 1135. (e) Majumder, S.; Odom, A. L. *Organometallics* **2008**, *27*, 1174. (f) Wood, M. C.; Leitch, D. C.; Yeung, C. S.; Kozak, J. A.; Schafer, L. L. *Angew. Chem., Int. Ed.* **2007**, *46*, 354. (g) Lee, A. V.; Schafer, L. L. *Eur. J. Inorg. Chem.* **2007**, 2243, and reference cited therein. (h) Gott, A. L.; Clarke, A. J.; Clarkson, G. J.; Scott, P. *Organometallics* **2007**, *26*, 1729. (i) Müller, C.; Loos, C.; Schulenberg, N.; Doye, S. *Eur. J. Org. Chem.* **2006**, 2499. (j) Watson, D. A.; Chiu, M.; Bergman, R. G. *Organometallics* **2006**, *25*, 4731. (k) Knight, P. D.; Munslow, I.; O'Shaughnessy, P. N.; Scott, P. *Chem. Commun.* **2004**, 894.
- (6) (a) Ackermann, L.; Kaspar, L. T.; Althammer, A. *Org. Biomol. Chem.* **2007**, *5*, 1975. (b) Schlummer, B.; Hartwig, J. F. *Org. Lett.* **2002**, *4*, 1471.
- (7) Komeyama, K.; Morimoto, T.; Takaki, K. *Angew. Chem., Int. Ed.* **2006**, *45*, 2938.
- (8) (a) Cochran, B. M.; Michael, F. E. *J. Am. Chem. Soc.* **2008**, *130*, 2786. (b) Cochran, B. M.; Michael, F. E. *Org. Lett.* **2008**, *10*, 329. (c) Michael, F. E.; Cochran, B. M. *J. Am. Chem. Soc.* **2006**, *128*, 4246.
- (9) (a) Bender, C. F.; Widenhoefer, R. A. *Chem. Commun.* **2006**, 4143. (b) Bender, C. F.; Widenhoefer, R. A. *Org. Lett.* **2006**, *8*, 5303. (c) Zhang, J.; Yang, C.-G.; He, C. J. *Am. Chem. Soc.* **2006**, *128*, 1798. (d) Liu, X.-Y.; Li, C.-H.; Che, C.-M. *Org. Lett.* **2006**, *8*, 2707. (e) Han, X.; Widenhoefer, R. A. *Angew. Chem., Int. Ed.* **2006**, *45*, 1747.
- (10) The Au-catalyzed intermolecular hydroamination of simple  $\alpha$ -olefins with cyclic ureas has been reported recently: Zhang, Z.; Lee, S. D.; Widenhoefer, R. A. *J. Am. Chem. Soc.* **2009**, *131*, 5372.
- (11) (a) Bender, C. F.; Widenhoefer, R. A. *J. Am. Chem. Soc.* **2005**, *127*, 1070. (b) Bender, C. F.; Hudson, W. B.; Widenhoefer, R. A. *Organometallics* **2008**, *27*, 2356.
- (12) Liu, Z.; Hartwig, J. F. *J. Am. Chem. Soc.* **2008**, *130*, 1570.
- (13) Bauer, E. B.; Andavan, G. T. S.; Hollis, T. K.; Rubio, R. J.; Cho, J.; Kuchenbeiser, G. R.; Helgert, T. R.; Letko, C. S.; Tham, F. S. *Org. Lett.* **2008**, *10*, 1175.
- (14) For our preliminary report of the use of  $[\text{Ir}(\text{COD})\text{Cl}]_2$  as a pre-catalyst for the intramolecular hydroamination of secondary alkyl- or arylamines (but not primary amines) and unactivated olefins, see: Hesp, K. D.; Stradiotto, M. *Org. Lett.* **2009**, *11*, 1449.
- (15) Ohmiya, H.; Moriya, T.; Sawamura, M. *Org. Lett.* **2009**, *11*, 2145.
- (16) Dorta, R. In *Iridium Complexes in Organic Synthesis*; Oro, L. A., Claver, C., Eds.; Wiley-VCH: Weinheim, 2009; p 145.
- (17) (a) Casalnuovo, A. L.; Calabrese, J. C.; Milstein, D. *J. Am. Chem. Soc.* **1988**, *110*, 6738. (b) Dorta, R.; Egli, P.; Zürcher, F.; Togni, A. *J. Am. Chem. Soc.* **1997**, *119*, 10857.
- (18) Zhou, J.; Hartwig, J. F. *J. Am. Chem. Soc.* **2008**, *130*, 12220.
- (19) For some recent reports, see: (a) Field, L. D.; Messerle, B. A.; Vuong, K. Q.; Turner, P. *Dalton Trans.* **2009**, 3599. (b) Ebrahimi, D.; Kennedy, D. F.; Messerle, B. A.; Hibbert, D. B. *Analyst* **2008**, *817*. (c) Burling, S.; Field, L. D.; Messerle, B. A.; Rumble, S. L. *Organometallics* **2007**, *26*, 4335. (d) Lai, R.-Y.; Surekha, K.; Hayashi, A.; Ozawa, F.; Liu, Y.-H.; Peng, S.-M.; Liu, S.-T. *Organometallics* **2007**, *26*, 1062. (e) Li, X.; Chianese, A. R.; Vogel, T.; Crabtree, R. H. *Org. Lett.* **2005**, *7*, 5437.

**Table 1.** Screening of Group 9 Catalyst Precursors for the Intramolecular Hydroamination of **1a** to Give **2a**<sup>a</sup>

entry	catalyst precursor	conversion to <b>2a</b> <sup>b</sup>
1–1	[Ir(COD)Cl] <sub>2</sub>	>95
1–2	[Ir(COE) <sub>2</sub> Cl] <sub>2</sub>	10
1–3	[Ir(COD)OMe] <sub>2</sub>	7
1–4	[( $\eta^5$ -C <sub>5</sub> Me <sub>5</sub> )IrCl <sub>2</sub> ] <sub>2</sub>	<5
1–5	[Rh(COD)Cl] <sub>2</sub>	<5
1–6	[Ir(COD) <sub>2</sub> ]BF <sub>4</sub>	<5
1–7	[Ir(MeCN) <sub>2</sub> (COD)]BF <sub>4</sub>	28 <sup>c</sup>
1–8	[Ir(COD)PCy <sub>3</sub> (py)]PF <sub>6</sub>	10 <sup>c</sup>
1–9	none	<5

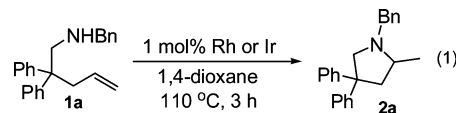
<sup>a</sup> Reaction Conditions: 0.25 mmol **1a** and 1.0 mol % Ir or Rh in 0.5 mL 1,4-dioxane at 110 °C for 3 h. <sup>b</sup> On the basis of <sup>1</sup>H NMR data (average of two runs); unless otherwise noted, **2a** was observed as the only reaction product. <sup>c</sup> Formation of **2a** was accompanied by other byproducts. COD =  $\eta^4$ -1,4-cyclooctadiene; COE = cyclooctene; Cy = cyclohexyl; py = pyridine.

intramolecular hydroamination of unactivated olefins. We provide herein a complete account of our studies using [Ir(COD)Cl]<sub>2</sub> as a precatalyst for the intramolecular addition of primary as well as secondary alkyl- or arylamines to unactivated olefins.<sup>14</sup> Mechanistic investigations of these intramolecular hydroamination reactions employing a combination of experimental and computational techniques reveal that such transformations proceed via an olefin activation mechanism that had previously not been documented for Ir-catalyzed alkene hydroamination.<sup>16–18</sup>

## Results and Discussion

**Catalyst Identification and Optimization.** The ability of simple group 9 complexes to mediate the intramolecular hydroamination of unactivated alkenes at relatively low catalyst loadings (1.0 mol % Rh or Ir) was surveyed by using the cyclization of the secondary alkylamine **1a** (eq 1) to the corresponding pyrrolidine **2a** in 1,4-dioxane (110 °C, 3 h) as a test reaction (Table 1). Under these conditions, the use of [Ir(COD)Cl]<sub>2</sub> as a precatalyst provided clean conversion to **2a** (<sup>1</sup>H NMR), and monitoring of the reaction revealed the transformation to be complete after 1 h. By comparison, other commercially available neutral Group 9 precatalysts performed poorly under these test conditions, including [Ir( $\eta^2$ -cyclooctene)<sub>2</sub>Cl]<sub>2</sub>, [Ir(COD)(OMe)]<sub>2</sub>, [( $\eta^5$ -C<sub>5</sub>Me<sub>5</sub>)IrCl<sub>2</sub>]<sub>2</sub>, and [Rh(COD)Cl]<sub>2</sub> (entries 1–2 to 1–5, respectively); inferior performance was also observed for the cationic Ir precatalysts [Ir(COD)<sub>2</sub>]BF<sub>4</sub>, [Ir(MeCN)<sub>2</sub>(COD)]BF<sub>4</sub>, and [Ir(COD)PCy<sub>3</sub>(pyridine)]PF<sub>6</sub> (Crabtree's catalyst) (entries 1–6 to 1–8, respectively). Further investigations revealed that the quantitative conversion of **1a** into **2a** can also be achieved by use of only 0.125 mol % [Ir(COD)Cl]<sub>2</sub> in 1,4-dioxane (3 h, 110 °C), or by employing higher Ir loadings at lower temperatures (2.5 mol % Ir; 7 h, 80 °C). While this reaction was also shown to proceed in 1,2-dichloroethane, 1,2-dimethoxyethane, or toluene, 1,4-dioxane proved to be the optimal solvent among those surveyed and was used for all subsequent catalytic studies (Table S1, Supporting Information). In keeping with the observation that the hydroamination of **1a** catalyzed by [Ir(COD)Cl]<sub>2</sub> exhibits an inverse-order rate dependence on the concentrations of each of **1a** and **2a** (*vide infra*), the conversion of **1a** to **2a** was found to be completely inhibited when employing 0.5 mol % [Ir(COD)Cl]<sub>2</sub> at 110 °C in 1,4-dioxane in the presence of an equivalent of K<sub>2</sub>CO<sub>3</sub> (relative to **1a**) or 1.0 mol % 1,8-diazabicyclo(5.4.0)undec-7-ene (DBU). While efforts to definitively characterize intermediates formed during

the [Ir(COD)Cl]<sub>2</sub>-mediated transformation of **1a** into **2a** (Ir:**1a** = 1:1) were thwarted by the relative complexity of the <sup>1</sup>H NMR spectra obtained under catalytically relevant conditions, it is worth noting that neither Ir-*H* nor Ir-*D* (when using **1a-d**<sub>1</sub> - the N-D isotopomer of **1a**) resonances were observed over a range of temperatures (25–80 °C) and throughout no free COD was detected (<sup>1</sup>H and <sup>2</sup>H NMR).



In an effort to further enhance the catalytic performance of [Ir(COD)Cl]<sub>2</sub>, the effect of added salts, as well as added phosphine coligands, was evaluated. In monitoring the transformation of **1a** to **2a**, the use of 0.25 mol % [Ir(COD)Cl]<sub>2</sub> as a precatalyst alone (110 °C) provided higher rates of conversion to **2a** than were achieved under analogous conditions when using 0.25 mol % [Ir(COD)Cl]<sub>2</sub> in the presence of 0.5 mol % N<sup>n</sup>Bu<sub>4</sub>Cl, LiOTf, AgBF<sub>4</sub>, or LiB(C<sub>6</sub>F<sub>5</sub>)<sub>4</sub>·2.5OEt<sub>2</sub> (Figure S1, Supporting Information); these results are surprising, given that increased catalytic activity is often observed for cationic late metal hydroamination catalysts when large, less-coordinating anions are employed.<sup>1a</sup> While for the hydroamination of **1a** the use of [Ir(COD)Cl]<sub>2</sub>/2 AgBF<sub>4</sub> as a precatalyst mixture afforded complete conversion (<sup>1</sup>H NMR) to **2a** after 3 h, the use of LiB(C<sub>6</sub>F<sub>5</sub>)<sub>4</sub>·2.5OEt<sub>2</sub> as a cocatalyst under similar conditions also generated a substantial amount of a byproduct arising from alkene isomerization within **1a**. In keeping with these observations, conductivity measurements of 1,4-dioxane solutions of [Ir(COD)Cl]<sub>2</sub> carried out under various conditions, including in the presence or absence of **1a**, as well as at room temperature or following preconditioning under catalytic conditions, provided no evidence for heterolytic Ir–Cl bond cleavage.

Given that the use of added phosphines has proven effective in promoting the intramolecular addition of secondary alkylamines to unactivated alkenes in reactions mediated by Rh,<sup>12</sup> Pt,<sup>11</sup> and Cu<sup>15</sup> precatalysts, the influence of such coligands on the catalytic performance of [Ir(COD)Cl]<sub>2</sub> in the cyclization of **1a** was surveyed. While no reactivity benefits were derived from the addition of phosphines in reactions conducted at 110 °C, the use of bulky R<sup>p</sup>Bu<sub>2</sub> phosphines (*R* = biaryl or ferrocenyl; Table S2, Supporting Information) did prove useful in promoting the formation of **2a** under more mild conditions than could be achieved by use of [Ir(COD)Cl]<sub>2</sub> alone. For example, while the use of 2.5 mol % [Ir(COD)Cl]<sub>2</sub> at 65 °C afforded 60% conversion to **2a** in the absence of byproduct over the course of 24 h, the incorporation of 5 mol % 2-(di-*t*-butylphosphino)-biphenyl (**L2**, Table S2, Supporting Information) as a coligand in this reaction afforded **2a** quantitatively (<sup>1</sup>H NMR) under similar reaction conditions. However, we were surprised to find that the rate of intramolecular hydroamination of **1a** employing [Ir(COD)Cl]<sub>2</sub>/**L2** catalyst mixtures exhibits an inverse-order dependence on **L2** at 65 °C and a zero-order rate dependence on **L2** at 110 °C (Figure S2, Supporting Information). On the basis of these data, it is unlikely that species featuring an Ir–P linkage represent important catalytic intermediates in the observed hydroamination of **1a**. Rather, the reactivity benefits of employing **L2** and related bulky phosphines at 65 °C may be attributable to the ability of such coligands to discourage the decomposition of catalytically inactive Ir intermediates, which in turn can serve as a source of catalytically active and



**Table 2.** Intramolecular Hydroamination of Unactivated Alkenes by Secondary Alkylamines Employing  $[\text{Ir}(\text{COD})\text{Cl}]_2$  as a Precatalyst<sup>a</sup>

entry	aminoalkene	product	mol % Ir (time, h)	yield <sup>b</sup>
2-1			0.25 (3)	88
2-2			1.0 (3)	85
2-3			1.0 (3)	87
2-4			2.5 (3)	89
2-5			1.0 (7)	88
2-6			2.5 (7)	86
2-7			5.0 (24)	84
2-8			2.5 (16)	92 (1.3:1) <sup>d</sup>
2-9			5.0 (24)	81 <sup>c</sup> (1.5:1) <sup>d</sup>
2-10			5.0 (24)	72 <sup>e</sup>
2-11			2.5 (16)	88
2-12			5.0 (48)	74
2-13			10 (48)	88
2-14			10 (48)	52 <sup>c</sup>

<sup>a</sup> Conditions: 0.25 mmol aminoalkene in 0.5 mL 1,4-dioxane at 110 °C; conversion to product >95% (<sup>1</sup>H NMR) unless stated. <sup>b</sup> Isolated percent yield unless stated (average of two runs). <sup>c</sup> <sup>1</sup>H NMR percent yield. <sup>d</sup> Diastereomeric ratio (dr, <sup>1</sup>H NMR). <sup>e</sup> Reaction run at 80 °C; conversion to the piperidine was 75% (<sup>1</sup>H NMR) with the balance corresponding to an alkene isomerization product.

phosphine-free Ir species. As such,  $[\text{Ir}(\text{COD})\text{Cl}]_2$  was employed for all subsequent catalytic studies without added coligands.

**Intramolecular Hydroamination of Secondary Alkylamines.** Encouraged by the ability of  $[\text{Ir}(\text{COD})\text{Cl}]_2$  to mediate the cyclization of **1a**, the hydroamination of alternative secondary alkylaminoalkene substrates, including those featuring polar groups, was examined (Table 2). The presence of halide (entry 2–2), ester (entry 2–3), or alkoxy (entry 2–4) substituents within the benzylamines **1b–d** did not significantly influence the progress of the reaction, and the bulky *N*-methylcyclohexyl aminoalkene **1e** was also cyclized (entry 2–5); in all cases, high isolated yields were obtained (85–89%) despite the use of relatively low catalyst loading (1–2.5 mol % Ir). Alternative *gem*-disubstituted relatives of **1a** also proved to be suitable hydroamination substrates (entries 2–6 to 2–8), as did the monosubstituted isopropyl-containing species featured in entry 2–9. The hexenylamine substrate featured in entry 2–10 was also efficiently cyclized in the presence of  $[\text{Ir}(\text{COD})\text{Cl}]_2$  to afford the corresponding piperidine derivative. In the pursuit of more difficult substrates, we turned our attention to the cyclohydroamination of unactivated disubstituted alkenes. While the use of  $[\text{Ir}(\text{COD})\text{Cl}]_2$  proved effective in promoting the cyclization of *gem*-disubstituted olefins (entries 2–11 and 2–12), hydroamination of the internal olefinic substrates featured in entries 2–13 and 2–14 presented a more significant challenge. Notably, throughout the course of these and the other  $[\text{Ir}(\text{COD})\text{Cl}]_2$ -mediated cyclohydroamination reactions reported

**Table 3.** Intramolecular Hydroamination of Unactivated Alkenes by Secondary Arylamines Employing  $[\text{Ir}(\text{COD})\text{Cl}]_2$  as a Precatalyst<sup>a</sup>

entry	aminoalkene	product	mol % Ir (time, h)	yield <sup>b</sup>
3-1			2.5 (7)	95
3-2			1.0 (7)	96
3-3			0.5 (7)	94
3-4			2.5 (7)	95
3-5			5.0 (24)	67 <sup>c</sup>
3-6			5.0 (16)	95
3-7			5.0 (16)	20 <sup>c,d</sup>
3-8			5.0 (24)	nr <sup>e</sup>

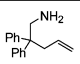
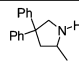
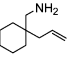
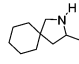
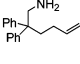
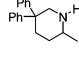
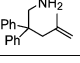
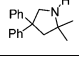
<sup>a</sup> Conditions: 0.25 mmol aminoalkene in 0.5 mL 1,4-dioxane at 110 °C; conversion to product >95% (<sup>1</sup>H NMR) unless stated. <sup>b</sup> Isolated percent yield unless stated (average of two runs). <sup>c</sup> <sup>1</sup>H NMR percent yield. <sup>d</sup> Conversion to the piperidine was 20% (<sup>1</sup>H NMR) with the balance corresponding to an alkene isomerization product. <sup>e</sup> No reaction of the aminoalkene was observed.

herein, no unsaturated hydroamination products arising from  $\beta$ -hydride elimination were detected.

In keeping with the  $\text{Cu}(\text{O}^t\text{Bu})/\text{Xantphos}$  catalyst system,<sup>15</sup> but in contrast to the  $\text{PtCl}_2/\text{biarylphosphine}$ <sup>11b</sup> and  $[\text{Rh}(\text{COD})_2]\text{BF}_4/\text{biarylphosphine}$ <sup>12</sup> catalyst systems, the use of  $[\text{Ir}(\text{COD})\text{Cl}]_2$  under our typical conditions (e.g., Table 2) proved ineffective in promoting the hydroamination of aminoalkene substrates lacking backbone substituents that promote cyclization. Furthermore, the *N*-Boc relative of **1a** (i.e., **1f**) proved unreactive (<sup>1</sup>H NMR) in the presence of  $[\text{Ir}(\text{COD})\text{Cl}]_2$  (Boc = *t*-butoxycarbonyl; 1.0 mol % Ir; 3 h, 110 °C). However, the observation that the cyclization of **1a** proceeds unhampered (<sup>1</sup>H NMR) when using a 1:1 mixture of **1a** and **1f** confirms that the latter does not poison the active catalyst derived from  $[\text{Ir}(\text{COD})\text{Cl}]_2$ . In this regard,  $[\text{Ir}(\text{COD})\text{Cl}]_2$  appears to be well-suited as a precatalyst for conducting chemoselective hydroaminations involving more complex organic molecules.

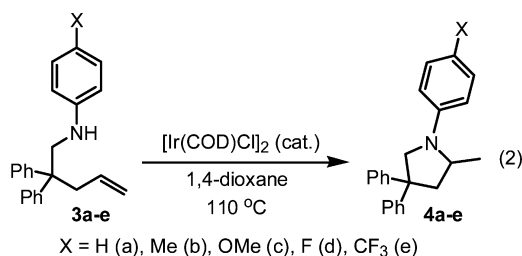
**Intramolecular Hydroamination of Secondary Arylamines.** The late metal-mediated cyclohydroamination of unactivated alkenes by secondary arylamines is limited to a single report featuring the cyclization of two simple *N*-Ph substrates.<sup>13</sup> The use of  $[\text{Ir}(\text{COD})\text{Cl}]_2$  as a precatalyst established expanded scope for this class of transformations (Table 3) in enabling the cyclization of the parent *N*-Ph substrate **3a** (entry 3–1), as well as for the first time arylaminoalkene substrates featuring *para* electron-donating (**3b** and **3c**; entries 3–2 and 3–3) and *para* electron-withdrawing (**3d** and **3e**; entries 3–4 and 3–5) substituents. While high isolated yields of **4a–d** were obtained for reactions conducted over the course of 7 h at 110 °C, the amount of catalyst needed to achieve quantitative conversion to **4** under these conditions varied significantly. Whereas only 0.25 mol %  $[\text{Ir}(\text{COD})\text{Cl}]_2$  was required to effect the clean hydroamination of the anisole derivative **3c** (entry 3–3), the use of 2.5 mol %  $[\text{Ir}(\text{COD})\text{Cl}]_2$  afforded only partial conversion of the trifluoromethyl species **3e** to **4e**, even after 24 h (entry 3–5); a more detailed kinetic analysis of these reactivity trends is provided (*vide infra*). Our observation that the intramolecular hydroamination of **3** is significantly enhanced by *para* electron-donating substituents (X in eq 2) is divergent from trends

**Table 4.** Intramolecular Hydroamination of Unactivated Alkenes by Primary Alkylamines Employing [Ir(COD)Cl]<sub>2</sub> and HNEt<sub>3</sub>Cl (1:2) as a Precatalyst Mixture<sup>a</sup>

entry	aminoalkene	product	mol % Ir (time, h)	yield <sup>b</sup>
4-1			5.0 (24)	89
4-2			5.0 (24)	75 <sup>c</sup>
4-3			5.0 (24)	84
4-4			10 (48)	87

<sup>a</sup> Conditions: 0.25 mmol aminoalkene in 0.5 mL 1,4-dioxane at 110 °C; conversion to product >95% (<sup>1</sup>H NMR) unless stated. <sup>b</sup> Isolated percent yield unless stated (average of two runs). <sup>c</sup> <sup>1</sup>H NMR percent yield; the remainder is attributed to an alkene isomerization product.

documented by Zhou and Hartwig,<sup>18</sup> who reported that both electron-rich and electron-poor anilines were less reactive than electron-neutral anilines toward the intermolecular hydroamination of activated bicyclic alkenes catalyzed by (bisphosphine)Ir species, which was shown to proceed by way of N–H bond activation/alkene insertion reaction pathway.<sup>18</sup> While an alternative backbone substitution pattern was tolerated (entry 3–6), the hydroamination of a 5-hexenyl substrate proceeded in low yield (entry 3–7), and efforts to promote the cyclization of the disubstituted olefinic substrate featured in entry 3–8 by use of [Ir(COD)Cl]<sub>2</sub> were unsuccessful. One might predict arylamine substrates to be inherently more susceptible to late metal-mediated hydroamination than alkylamines; the lower basicity of the former should reduce catalyst inhibition arising from unproductive substrate and/or product binding, and should also serve to promote N–H bond cleavage in hydroamination reactions involving net proton transfer from nitrogen. However, a comparative reactivity survey revealed that some of the most effective late metal catalysts known for the intramolecular hydroamination of unactivated alkenes fail to promote the cyclization of arylamines such as **3a**.<sup>14</sup>



**Intramolecular Hydroamination of Primary Amines.** The cyclohydroamination of unactivated alkenes with primary amines provides an atom-economical synthetic route to N–H containing cyclic secondary amines which, unlike alternative protocols, circumvents the installation and removal of nitrogen protecting groups. Although transformations of this type are well established for several classes of hydroamination catalysts,<sup>1a</sup> the late metal-mediated cyclization of such substrates has been achieved only recently by use of [Rh(COD)<sub>2</sub>]BF<sub>4</sub>/biarylphosphine<sup>12</sup> or Cu(O<sup>*i*</sup>Bu)/Xantphos.<sup>15</sup> Our initial efforts to effect the cyclization of the primary aminoalkenes featured in Table 4 by using [Ir(COD)Cl]<sub>2</sub> as a precatalyst under a variety of experimental conditions were unsuccessful. However, the knowledge

that Brønsted acids can act as catalysts<sup>6</sup> or cocatalysts<sup>20</sup> in promoting the intramolecular hydroamination of unactivated alkenes and alkynes provided the motivation to examine the use of [Ir(COD)Cl]<sub>2</sub>/Brønsted acid catalyst mixtures. To the best of our knowledge, the Brønsted acid-mediated intramolecular hydroamination of unactivated alkenes with primary amines is limited to a single example by Ackermann and co-workers,<sup>6a</sup> in which the cyclization of the substrate featured in entry 4–1 (Table 4) was achieved in 83% yield by use of 20 mol % [PhMe<sub>2</sub>NH]B(C<sub>6</sub>F<sub>5</sub>)<sub>4</sub> (18 h, 120 °C). In the pursuit of a more convenient and cost-effective cocatalyst, HNEt<sub>3</sub>Cl and CF<sub>3</sub>SO<sub>3</sub>H<sup>6b</sup> were each evaluated. While none of 2.5 mol % [Ir(COD)Cl]<sub>2</sub>, 10 mol % HNEt<sub>3</sub>Cl, and 10 mol % CF<sub>3</sub>SO<sub>3</sub>H individually proved capable of promoting the hydroamination of the primary aminoalkene substrates featured in Table 4 (24 h, 110 °C), the use of 2.5 mol % [Ir(COD)Cl]<sub>2</sub>/5 mol % HNEt<sub>3</sub>Cl as a precatalyst mixture provided excellent conversions to the targeted N–H containing cyclic secondary amines. Inferior results were obtained, including the formation of byproducts, when 5 mol % CF<sub>3</sub>SO<sub>3</sub>H was used as a cocatalyst under similar conditions. Control experiments confirmed that neither 10 mol % N<sup>*n*</sup>Bu<sub>4</sub>Cl nor mixtures comprised of 2.5 mol % [Ir(COD)Cl]<sub>2</sub>/5 mol % N<sup>*n*</sup>Bu<sub>4</sub>Cl are capable of promoting the cyclization of these substrates under our experimental conditions. The catalytic performance of [Ir(COD)Cl]<sub>2</sub>/HNEt<sub>3</sub>Cl in the cyclization of these primary aminoalkene substrates is competitive with that of the previously reported “two-component” late metal catalysts [Rh(COD)<sub>2</sub>]BF<sub>4</sub>/biarylphosphine<sup>12</sup> and Cu(O<sup>*i*</sup>Bu)/Xantphos.<sup>15</sup>

**Kinetic Studies.** A number of distinct mechanistic pathways have been uncovered for the hydroamination of alkenes.<sup>1</sup> In the case of late metal-mediated transformations these include (but are not restricted to) processes involving: nucleophilic attack of an amine on a metal-coordinated alkene,<sup>8,11,21</sup> an  $\eta^3$ -allyl or related complex,<sup>22</sup> or an  $\eta^6$ -vinylarene complex;<sup>23</sup> N–H bond activation followed by alkene insertion into an M–NR<sub>2</sub> linkage;<sup>16–18</sup> amine coordination followed by proton-transfer to an activated alkene;<sup>24</sup> and nucleophilic attack of a metal amido species on an activated alkene.<sup>25</sup> While experimental evidence for Ir-mediated N–H bond activation/alkene insertion reaction sequences has been obtained for the intermolecular hydroamination of activated alkenes such as norbornene,<sup>16–18</sup> mechanistic experiments indicate that the Ir-catalyzed intramolecular hydroamination (and hydroalkoxylation) of alkynes can proceed via alternative reaction pathways involving alkyne activation/nucleophilic attack.<sup>19e,26</sup> However, a thorough kinetic analysis of the late metal-mediated cyclohydroamination of

- (20) (a) Bender, C. F.; Widenhoefer, R. A. *Chem. Commun.* **2008**, 2741. (b) Penzien, J.; Su, R. Q.; Müller, T. E. *J. Mol. Catal., A* **2002**, 182–183, 489. (c) Müller, T. E.; Berger, M.; Grosche, M.; Herdtweck, E.; Schmidtchen, F. P. *Organometallics* **2001**, 20, 4384.
- (21) Kovács, G.; Ujaque, G.; Lledós, A. *J. Am. Chem. Soc.* **2008**, 130, 853.
- (22) (a) Sakai, N.; Ridder, A.; Hartwig, J. F. *J. Am. Chem. Soc.* **2006**, 128, 8134. (b) Johns, A. M.; Utsunomiya, M.; Incarvito, C. D.; Hartwig, J. F. *J. Am. Chem. Soc.* **2006**, 128, 1828. (c) Pawlas, J.; Nakao, Y.; Kawatsura, M.; Hartwig, J. F. *J. Am. Chem. Soc.* **2002**, 124, 3669. (d) Vo, L. K.; Singleton, D. A. *Org. Lett.* **2004**, 6, 2469. (e) Nettekoven, U.; Hartwig, J. F. *J. Am. Chem. Soc.* **2002**, 124, 1166.
- (23) Takaya, J.; Hartwig, J. F. *J. Am. Chem. Soc.* **2005**, 127, 5756.
- (24) McBee, J. L.; Bell, A. T.; Tilley, T. D. *J. Am. Chem. Soc.* **2008**, 130, 16562.
- (25) (a) Leighton-Munro, C.; Delp, S. A.; Alsop, N. M.; Blue, E. D.; Gunnoe, T. B. *Chem. Commun.* **2008**, 111. (b) Leighton-Munro, C.; Delp, S. A.; Blue, E. D.; Gunnoe, T. B. *Organometallics* **2007**, 26, 1483.
- (26) Genin, E.; Antoniotti, S.; Michelet, V.; Genêt, J.-P. *Angew. Chem., Int. Ed.* **2005**, 44, 4949.

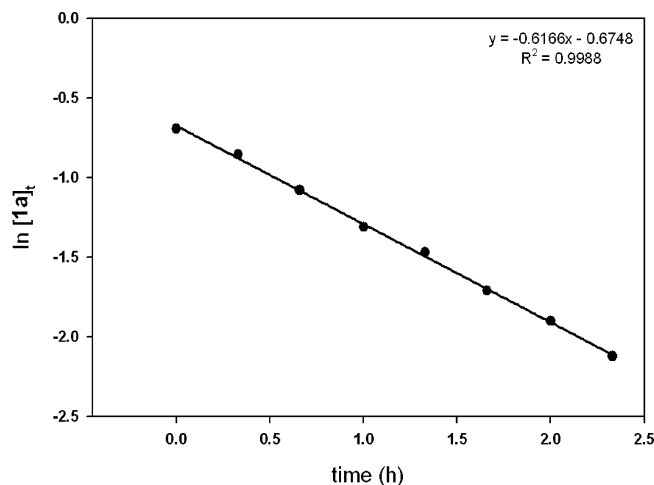


**Figure 1.** Representative plot for the conversion of **1a** to **2a** catalyzed by  $[\text{Ir}(\text{COD})\text{Cl}]_2$ . The reactions were conducted in 1,4-dioxane at 110 °C at the following concentrations:  $[\text{Ir}] = 5.0 \times 10^{-6}$  M and  $[\mathbf{1a}] = 5.0 \times 10^{-4}$  M.

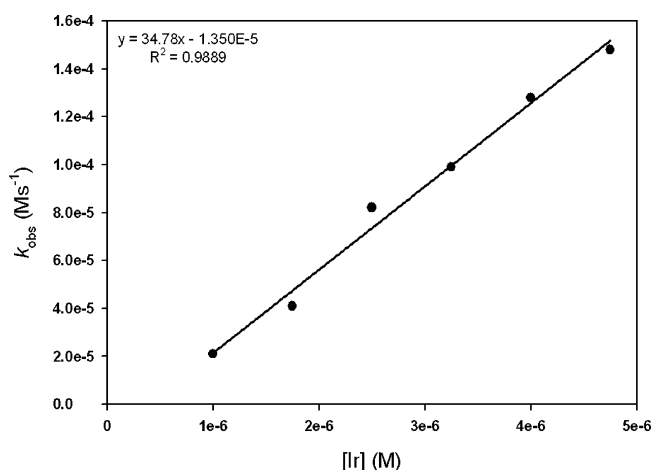


**Figure 2.** Relationship between  $k_{\text{obs}}$  and  $[\text{Ir}]$ . The reactions were conducted in 1,4-dioxane at 110 °C at the following concentrations:  $[\mathbf{1a}] = 5.0 \times 10^{-4}$  M and  $[\text{Ir}] = 1.0 \times 10^{-6}$  M to  $4.75 \times 10^{-6}$  M.

unactivated alkenes with secondary alkyl- or arylamines has yet to appear in the literature. In an effort to gain insight into the mechanism of such transformations, so as to guide the development of increasingly effective catalysts, a kinetic examination of the  $[\text{Ir}(\text{COD})\text{Cl}]_2$ -mediated hydroamination reactions featured herein was conducted.

**Kinetic Order of the Reaction.** Kinetic parameters were obtained for the hydroamination of **1a** catalyzed by  $[\text{Ir}(\text{COD})\text{Cl}]_2$ ; pseudofirst order rate constants were determined by monitoring the disappearance and appearance of **1a** and **2a**, respectively, relative to an internal standard over the course of 2–3 half-lives ( $^1\text{H}$  NMR; Figure 1). We first examined the order of reaction in  $[\text{Ir}(\text{COD})\text{Cl}]_2$  by combining **1a** (0.5 mM) with varied concentrations of  $[\text{Ir}]$  (0.001 to 0.00475 mM) in 1,4-dioxane at 110 °C. As shown in Figure 2, a plot of reaction rate ( $k_{\text{obs}}$ ) versus  $[\text{Ir}]$  was linear, indicating a first-order kinetic dependence on catalyst. This observation is consistent with a mechanism involving a monomeric Ir catalyst species, and would appear to preclude slow dissociation of a dimeric precatalyst to an active monomer. Further confirmation of a first-order dependence was provided by a nonlinear least-squares fit

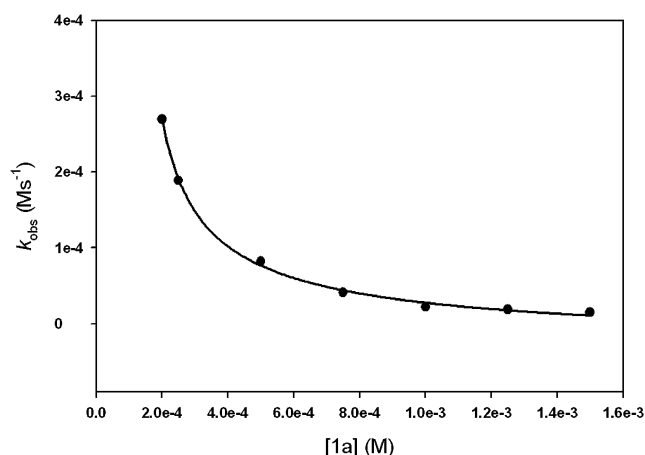


**Figure 3.** Relationship between  $k_{\text{obs}}$  and **1a**. The reactions were conducted in 1,4-dioxane at 110 °C at the following concentrations:  $[\text{Ir}] = 2.5 \times 10^{-6}$  M and  $[\mathbf{1a}] = 2.0 \times 10^{-4}$  M to  $1.5 \times 10^{-3}$  M.

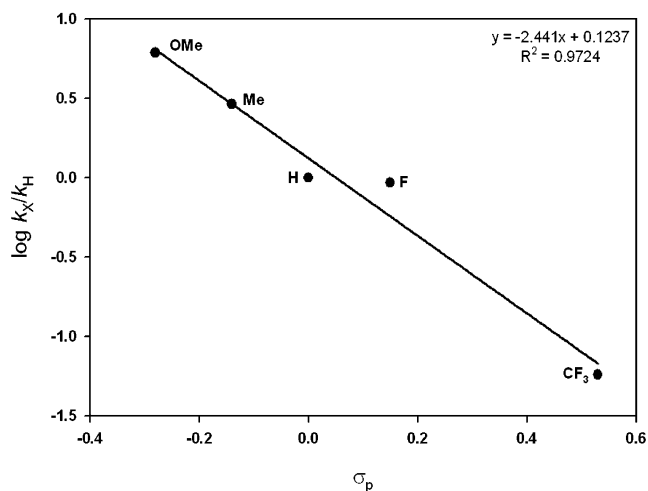


**Figure 4.** Hammett plot for the  $[\text{Ir}(\text{COD})\text{Cl}]_2$  catalyzed hydroamination of arylamines **3a–e**. The reactions were conducted in 1,4-dioxane at 110 °C at the following concentrations:  $[\mathbf{3a–e}] = 5.0 \times 10^{-4}$  M and  $[\text{Ir}] = 5.0 \times 10^{-6}$  M.

to  $f(x) = a[\text{Ir}]^n$ , which provided an order ( $n$ ) of 1.15(9) (Figure S4b, Supporting Information).

The kinetic order in **1a** was investigated subsequently by using a constant  $[\text{Ir}]$  (0.0025 mM) along with a  $[\mathbf{1a}]$  ranging from 0.25 to 1.5 mM in 1,4-dioxane at 110 °C. In keeping with the findings of Cochran and Michael,<sup>8a</sup> we observed decreasing reaction rates with increased initial concentrations of **1a**, which is consistent with an inverse order dependence of the rate of reaction on substrate concentration (Figure 3). Furthermore, the rate of cyclization of **1a** was observed to decrease by approximately 50% when measured in the presence of an equivalent of added **2a**. These results demonstrate both competitive substrate and product inhibition. While on the basis of these kinetic data alone we are unable to comment definitively regarding the mode of catalyst inhibition by **1a** and **2a**, possible scenarios that can be envisioned include (but are not restricted to) unproductive binding of **1a** or **2a** to Ir, as well as deprotonation of an amine/ammonium intermediate<sup>8b</sup> by **1a** or **2a**. However, computational studies support catalyst inhibition by **1a** and **2a** arising from the latter deprotonation pathway (*vide infra*).

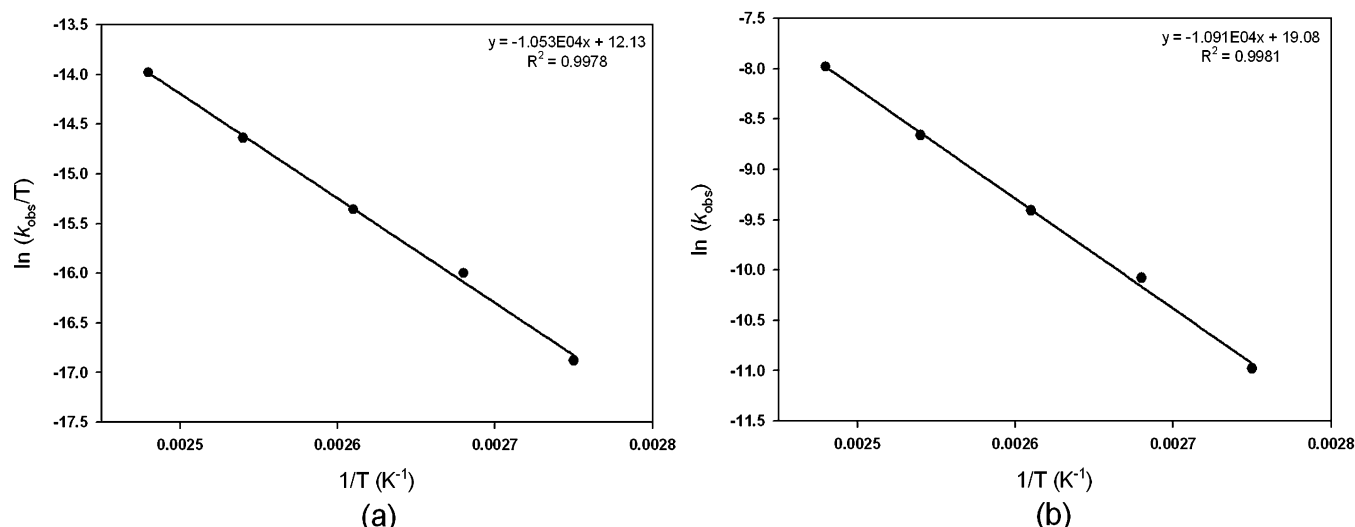
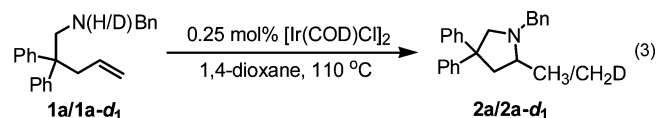


**Figure 5.** (a) Eyring plot for the hydroamination of **1a** catalyzed by [Ir(COD)Cl]<sub>2</sub>. The reactions were conducted in 1,4-dioxane over a temperature range of 90–130 °C at the following concentrations: [**1a**] =  $5.0 \times 10^{-4}$  M and [Ir] =  $2.5 \times 10^{-6}$  M ( $\Delta H^\ddagger = 20.9(3)$  kcal mol<sup>-1</sup>,  $\Delta S^\ddagger = -23.1(8)$  cal/K·mol). (b) Arrhenius plot for the hydroamination of **1a** catalyzed by [Ir(COD)Cl]<sub>2</sub>. The reactions were conducted in 1,4-dioxane over a temperature range of 90–130 °C at the following concentrations: [**1a**] =  $5.0 \times 10^{-4}$  M and [Ir] =  $2.5 \times 10^{-6}$  M ( $E_a = 21.6(3)$  kcal mol<sup>-1</sup>).

**Hammett Study.** The rate of the [Ir(COD)Cl]<sub>2</sub>-catalyzed hydroamination of **3a–e** was examined as a function of the *para*-substituent (X) on the arylamine (eq 2). The cyclization of **3a–e** (Table 3, entries 3–1 to 3–5) in the presence of 0.5 mol % [Ir(COD)Cl]<sub>2</sub> was monitored by use of <sup>1</sup>H NMR methods to obtain reaction rates. A Hammett plot of the resulting data provided a large, negative  $\rho$  value of  $-2.4(2)$  (Figure 4), which indicates that more electron-rich arylamines undergo hydroamination more rapidly.

**Kinetic Isotope Effect.** To provide some insight into the turnover-limiting step of the mechanism, the H/D kinetic isotope effect (KIE) for the [Ir(COD)Cl]<sub>2</sub>-catalyzed hydroamination **1a** was measured under catalytic conditions. The pseudofirst order plots (Figure S7, Supporting Information) of the cyclization of **1a** and **1a-d<sub>1</sub>** in 1,4-dioxane at 110 °C (eq 3) provided  $k_{\text{obs}} = 0.30(1)$  h<sup>-1</sup> and  $k_{\text{obs}} = 0.089(2)$  h<sup>-1</sup>, respectively, which translated to a primary KIE of 3.4(3). While these observations implicate the hydrogen derived from the N–H of **1a** in the rate-determining step, several competing reaction pathways (e.g., rate-limiting N–H oxidative addition or proton transfer following nucleophilic attack on a coordinated alkene) that account for these observations can be envisioned.



**Activation Parameters.** To obtain activation parameters for the [Ir(COD)Cl]<sub>2</sub>-catalyzed hydroamination of **1a**, a series of reactions were executed over a range of temperatures (90 – 130 °C); pseudofirst order rate constants were obtained from linear plots of [**1a**]<sub>t</sub> versus time over this temperature range. Eyring and Arrhenius analyses for the cyclization of **1a** to **2a** afforded  $\Delta H^\ddagger = 20.9(3)$  kcal mol<sup>-1</sup>,  $\Delta S^\ddagger = -23.1(8)$  cal/K·mol, and  $E_a = 21.6(3)$  kcal mol<sup>-1</sup> (Figure 5). The observation of a

large negative  $\Delta S^\ddagger$  value in the cyclization **1a** mediated by [Ir(COD)Cl]<sub>2</sub> is consistent with a highly ordered transition state.<sup>27</sup>

**Summary of Kinetic Experiments.** Kinetic analyses of the [Ir(COD)Cl]<sub>2</sub>-catalyzed hydroamination of **1a** have revealed that the reaction rate shows first order dependence on the concentration of Ir and inverse order dependence with respect to both substrate (**1a**) and product (**2a**) concentrations. While the observed primary kinetic isotope effect ( $k_{\text{H}}/k_{\text{D}} = 3.4(3)$ ) and the observation that increased electron density at nitrogen in **3** promotes the cyclization of these arylaminoalkene substrates ( $\rho = -2.4$ ) are in keeping with an alkene activation mechanism involving nucleophilic attack of a tethered amine on a metal-coordinated alkene followed by a rate-limiting protonolysis step, alternative mechanisms including those involving N–H oxidative addition cannot be ruled out on the basis of these empirical data alone. Given the lack of spectroscopic evidence that would enable the definitive identification of catalytic intermediates in the present study (*vide supra*), and in an effort to gain further insight into the elusive details of the mechanism of the [Ir(COD)Cl]<sub>2</sub>-catalyzed cyclohydroamination of unactivated aminoalkenes, this process was subjected to computational examination.

**Computational Study.** The DFT method has been employed as an established and predictive means to aid mechanistic understanding; the particular value of such methods for unraveling intricacies of hydroamination catalysis has been demonstrated previously by several groups.<sup>28–31</sup> Plausible mechanistic scenarios employing [Ir(COD)Cl]<sub>2</sub> as a precatalyst involving either activation of the alkene linkage (C=C bond activation

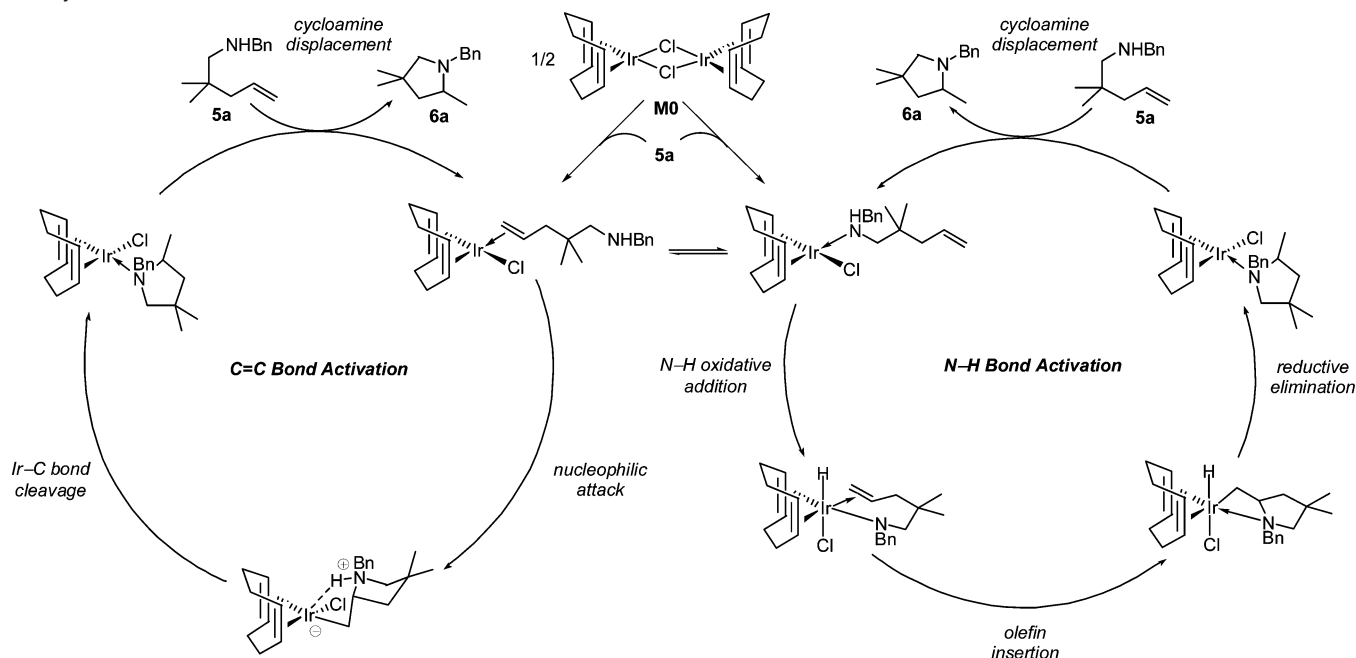
(27) Anslyn, E. V.; Dougherty, D. A. *Modern Physical Organic Chemistry*, 1st ed.; University Science Books: Sausalito, 2006; p 372.

(28) For a computational study of group 8 metal-assisted intermolecular hydroamination, see: (a) Senn, H. M.; Blöchl, P. E.; Togni, A. *J. Am. Chem. Soc.* **2000**, *122*, 4098. (b) Tsipis, C. A.; Kefaldis, C. E. *Organometallics* **2006**, *25*, 1696. (c) Tsipis, C. A.; Kefaldis, C. E. *J. Organomet. Chem.* **2007**, *692*, 5245.

(29) For a computational study of group 4 metal-assisted intermolecular hydroamination, see: Straub, B. F.; Bergman, R. G. *Angew. Chem., Int. Ed.* **2001**, *40*, 4632.



**Scheme 1.** Plausible Mechanistic Pathways for Late Transition Metal-Catalyzed Cyclohydroamination, Exemplified for  $[\text{Ir}(\text{COD})\text{Cl}]_2$  **M0** as Catalyst Precursor and **5a** as Substrate



route, Scheme 1, left)<sup>32</sup> or of the amine functionality (N–H bond activation route, Scheme 1, right)<sup>33</sup> have been examined for the cyclohydroamination of *N*-benzyl-2,2-dimethyl-4-en-1-amine **5a** (representing a prototypical secondary alkylamine) into the pyrrolidine **6a** (entry 2–7 in Table 2). Notably, this represents the first attempt to comprehensively address the mechanism of intramolecular hydroamination mediated by late transition metal compounds by means of computational methods. No structural simplification of any of the key species has been imposed. While the presentation herein is focused exclusively

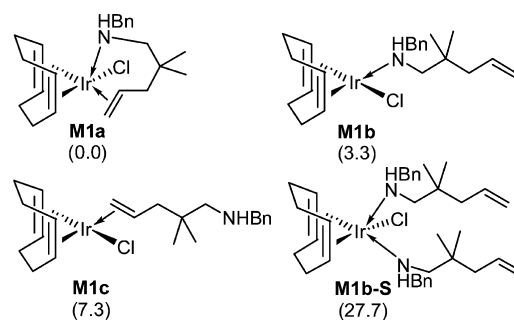


**Figure 6.** Various forms of the catalytically competent compound **M1** (free energy in kcal mol<sup>−1</sup> relative to **M1a**).

on the most accessible pathways, a complete account of all scrutinized species is given in the Supporting Information.<sup>34</sup>

**Nature of the Catalytically Competent Species.** We start by examining the fragmentation of precatalyst **M0** in the presence of substrate **5a** and 1,4-dioxane solvent,<sup>35</sup> which leads to the catalytically competent species. DFT predicts that  $[\text{Ir}(\text{COD})\text{Cl}(\text{substrate})]$  complex **M1** is predominantly generated in a transformation that is slightly downhill ( $\Delta G = -3.1$  kcal mol<sup>−1</sup> for  $1/2\text{M0} + 5a \rightarrow \text{M1a}$ ), while  $[\text{Ir}(\text{COD})\text{Cl}(\text{dioxane})]$  **M1\*** and dioxane or substrate adducts of **M1** or **M1\*** (respectively) are distinctly disfavored thermodynamically.<sup>34</sup> Compound **M1** is present in several forms featuring a chelating aminoalkene (**M1a**), or a monohapto association to the Ir<sup>I</sup> center through its amine (**M1b**) or olefin (**M1c**) functionalities, all of which are in rapid equilibrium (Figure 6).<sup>36</sup> Although **M1a** is most stable, it does not represent the direct precursor for cyclohydroamination proceeding through rival routes for olefin or N–H bond

- (30) For computational studies of group 4 transition metal-assisted intramolecular hydroamination of various substrate classes, see: aminoalkene substrates: (a) Müller, C.; Koch, R.; Doye, S. *Chem.—Eur. J.* **2008**, *14*, 10430. aminoallene substrates: (b) Tobisch, S. *Dalton Trans.* **2006**, 4277. (c) Tobisch, S. *Chem.—Eur. J.* **2007**, *13*, 4884. (d) Tobisch, S. *Chem.—Eur. J.* **2008**, *14*, 8590.
- (31) For computational studies of organolanthanide-assisted intramolecular hydroamination of various substrate classes, see: aminoalkene substrates: (a) Motta, A.; Lanza, G.; Fraga, I. L. *Organometallics* **2004**, *23*, 4097. aminoalkyne substrates: (b) Motta, A.; Lanza, G.; Fraga, I. L. *Organometallics* **2006**, *25*, 5533. aminoallene substrate: (c) Tobisch, S. *Chem.—Eur. J.* **2006**, *12*, 2520. aminodiene substrates: (d) Tobisch, S. *J. Am. Chem. Soc.* **2005**, *127*, 11979. (e) Tobisch, S. *Chem.—Eur. J.* **2007**, *13*, 9127.
- (32) For a selection of lead references for the olefin activation route, see: (a) Kiji, J.; Nishimura, S.; Yoshikawa, S.; Sasakawa, E.; Furukawa, J. *Bull. Chem. Soc. Jpn.* **1974**, *47*, 2523. (b) Armbrüch, J.; Pregosin, P. S.; Venanzi, L. M.; Consiglio, G.; Bachechi, F.; Zambonelli, L. J. *Organomet. Chem.* **1979**, *181*, 255. (c) Seligson, A. L.; Troglor, W. C. *Organometallics* **1993**, *12*, 744. (d) Kwatsura, M.; Hartwig, J. F. *J. Am. Chem. Soc.* **2000**, *122*, 9646. (e) Müller, T. E.; Grosche, M.; Herdtweck, E.; Pleier, A.-K.; Walter, E.; Yan, Y.-K. *Organometallics* **2000**, *19*, 170. (f) Seul, J. M.; Park, S. J. *Chem. Soc., Dalton Trans.* **2002**, 1153. (g) Karshtedt, D.; Bell, A. T.; Tilley, T. D. *J. Am. Chem. Soc.* **2005**, *127*, 12640. (h) References 19e and 20c herein.
- (33) For a selection of lead references for the amine activation route, see: (a) Casalnuovo, A. L.; Calabrese, J. C.; Milstein, D. *Inorg. Chem.* **1987**, *26*, 971. (b) Cowan, R. L.; Troglor, W. C. *Organometallics* **1987**, *6*, 2451. (c) Park, S.; Johnson, M. P.; Roundhill, D. M. *Organometallics* **1989**, *8*, 1700. (d) Ladipo, F. T.; Merola, J. S. *Inorg. Chem.* **1990**, *29*, 4127. (e) Koelliker, R.; Milstein, D. *Angew. Chem., Int. Ed. Engl.* **1991**, *30*, 707. (f) Glueck, D. S.; Newman Winslow, L. J.; Bergman, R. G. *Organometallics* **1991**, *10*, 1461. (g) Seligson, A. L.; Cowan, R. L.; Troglor, W. C. *Inorg. Chem.* **1991**, *30*, 3371. (h) References 16–18 herein.

(34) See the Supporting Information for more detail.

(35) The activation energy for fragmentation of **M0** has not been assessed, but it is rather unlikely to invoke any significant barrier, as the examination by a linear-transition approach gave no indication for the existence of such a barrier.

(36) Examination by a linear-transition approach gave no indication that this process is associated with a substantial enthalpy barrier.



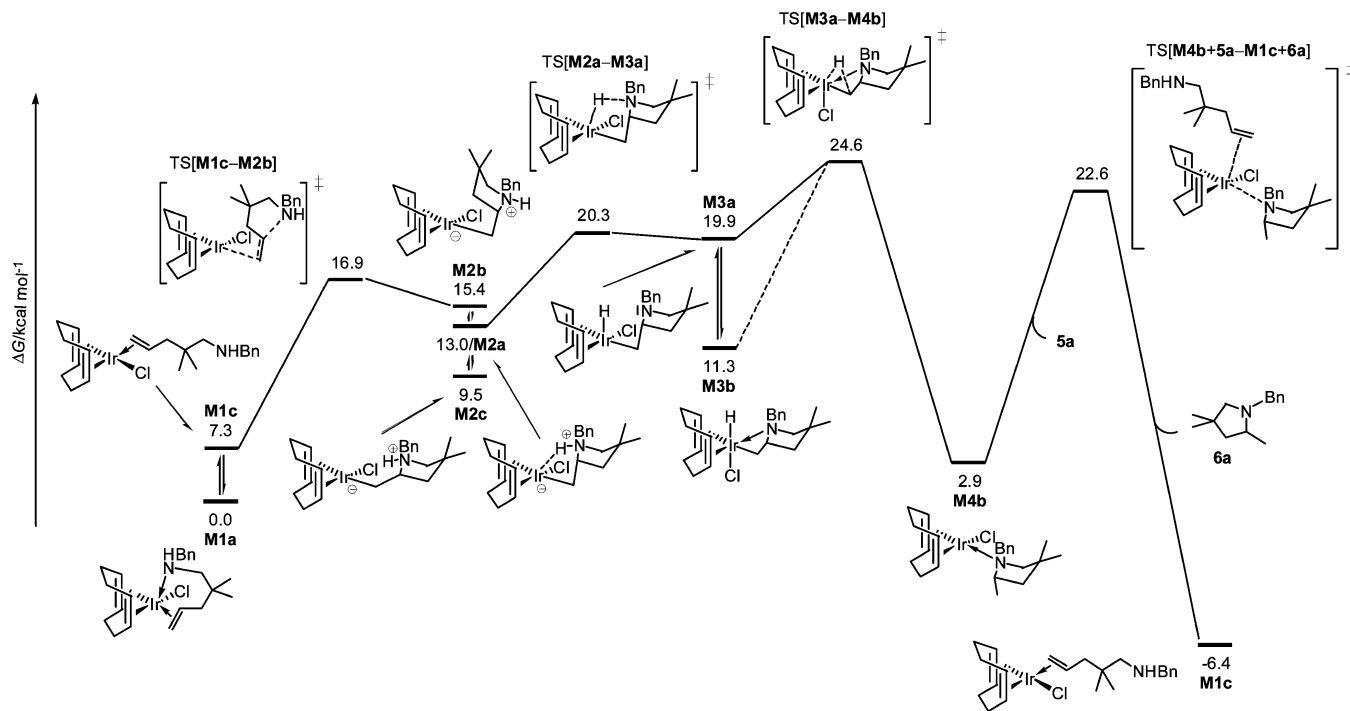


**Figure 7.** Free energy profile for the intramolecular hydroamination of **5a** by [Ir(COD)Cl]<sub>2</sub> (**M0**) proceeding via C=C bond activation. Only the most accessible pathway for all principal steps is shown, while alternative, but less favorable pathways are omitted for the sake of clarity.

activation (*vide infra*). Notably, the energetic cost of associating a second equivalent of substrate as in **M1b-S** suggests that substrate inhibition via formation of [Ir(COD)(substrate)<sub>2</sub>]Cl species is unlikely.

The observed similarities in hydroamination of **1a** mediated by [Ir(COD)Cl]<sub>2</sub> and [Ir(COD)Cl]<sub>2</sub>/2 AgBF<sub>4</sub> (*vide supra*) may argue in favor of a formally cationic complex as representing the active catalyst species. We have therefore probed the aptitude of the dioxane solvent to support the displacement of the chloride from the immediate proximity of the Ir center.<sup>37</sup> Given the low acceptor number of dioxane, it comes as no surprise that a [Ir(COD)(substrate)(dioxane)]Cl solvent-separated ion pair is found to be distinctly less stable than **M1**, being uphill by more than 28 kcal mol<sup>-1</sup>,<sup>34</sup> which corroborates the conductivity measurements (*vide supra*). Thus, our combined experimental and computational approach provides compelling evidence for **M1** as being the catalytically competent compound.

**Hydroamination via C=C Bond Activation.** Principal steps of the C=C bond activation route include: (1) nucleophilic attack of the amine on the olefin functionality, which is activated by coordination to the Ir center, to form a zwitterionic Ir<sup>I</sup>-cycloammonio-alkyl intermediate; (2) net protonolysis of the Ir–C bond; and (3) displacement of cycloamine by a new substrate molecule to regenerate **M1**. Figure 7 shows the Gibbs free-energy profile, which considers only the most accessible reaction pathways.<sup>34</sup>

The C–N bond forming step can proceed through distinct trajectories constituting frontside (i.e., amine approach *cis(syn)* to the metal) and backside (i.e., amine approach *trans(anti)* to the metal) attacks, thereby giving rise to various conformers of the zwitterionic Ir<sup>I</sup>-cycloammonio-alkyl intermediate **M2** (see Figure 7). The *cis(syn)* amine attack on the olefin unit initially

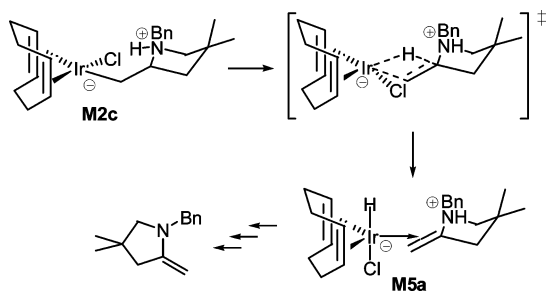
gives rise to **M2a**, which has the hydrogen of the quarternized ammonium center placed closely to the Ir<sup>I</sup> center, while the approach from backside leads first to **M2b**. Both transient intermediates **M2a** and **M2b** relax almost instantaneously into the minimum-energy conformer **M2c**,<sup>36</sup> featuring a positively charged ammonium unit that points toward the negatively polarized chlorine. Intramolecular C–N bond formation does preferably proceed via external attack of the amine unit on the coordinated double bond and commences from **M1c** as the direct precursor species, such that the amine group must first disconnect from the Ir center in the prevalent isomer **M1a** prior to cyclization. Both trajectories are found to be viable, with backside attack emerging as the dominant pathway in a process that is uphill and features a moderate activation barrier ( $\Delta G^\ddagger = 16.9$  kcal mol<sup>-1</sup>), thereby indicating that ring closure is smooth and reversible.

Several scenarios for cleavage of the Ir–C bond in **M2** have been probed, including: (a) direct protonolysis by the proton available from the ammonium unit; and (b) proton transfer to the Ir center, affording the Ir<sup>III</sup>-hydrido-cycloamido intermediate **M3**, with subsequent C–H reductive elimination of the cycloamine.<sup>34</sup> The stepwise mechanism via transient **M3** represents the kinetically advantageous scenario. The most accessible pathway commences from **M2a**,<sup>38</sup> which has the ammonium unit already suitably oriented toward the Ir center, such that its deprotonation does not cause major structural reorganization. Moreover, the nucleophilicity of the Ir<sup>I</sup> center supports this transformation electronically. Indeed, the **M2a** → **M3a** proton transfer has a low barrier of only 10.8 kcal mol<sup>-1</sup> (relative to the most stable **M2c**) to overcome and leads directly to the square-pyramidal **M3a** bearing the hydride in the apical position.

(37) This was done by employing a discrete ensemble of three molecules of 1,4-dioxane closely interacting with the Cl center, thereby simulating specific solvation effects adequately.

(38) The various conformers of the zwitterionic intermediate **M2** are in rapid equilibrium, as mutual interconversion does not impose any substantial barrier due to almost free rotation of the azacycle unit around Ir–C and C–C bonds in **M2**.

**Scheme 2.**  $\beta$ -Hydride Elimination as a Rival Event for the C=C Bond Activation Route



**M3a** represents a very shallow minimum on the free-energy surface (with  $\Delta G^\ddagger = 0.4$  kcal mol<sup>-1</sup> for reverse **M3a**  $\rightarrow$  **M2a**), thereby implicating an almost negligible stationary population, which would make **M3a** rather difficult to observe by use of NMR spectroscopic techniques (*vide supra*). Transient **M3a** can undergo skeletal rearrangement<sup>39</sup> to afford six-coordinate **M3b** as the most stable form of the Ir<sup>III</sup>-hydrido complex, having Cl and H in trans positions and the azacycle's N donor center directly attached to the metal (Figure 7). Notably, the transition state (TS) structure traversed along the most accessible pathway for reductive elimination adopts the same ligand arrangement. Given the small energy gap between the initially formed **M3a** and the lowest-energy TS for reductive elimination, it can reasonably be assumed that skeletal rearrangement in **M3a** and ensuing reductive elimination do occur concomitantly. Accordingly, C–H bond reductive elimination to commence from five-coordinate **M3a** proceeds through a highly ordered six-coordinate TS structure and affords the Ir<sup>I</sup>-pyrrolidine compound **M4b**. The associated low barrier ( $\Delta G^\ddagger = 4.7$  kcal mol<sup>-1</sup>) together with the substantial thermodynamic force ( $\Delta G = 17.0$  kcal mol<sup>-1</sup>) is in keeping with **M3a** as being a high-energy reactive intermediate. The reductive elimination has the higher total barrier (i.e., relative to **M1a**) of the two consecutive steps and thus discriminates the overall kinetics of the stepwise cleavage of the Ir–C bond in **M2**. Thereafter, incoming substrate displaces the pyrrolidine **6a** from **M4b** and regenerates the **M1c** active species, which re-enters the catalytic cycle. The exchange of cycloamine by substrate is thermodynamically favorable ( $\Delta G = -9.3$  kcal mol<sup>-1</sup>) and kinetically viable ( $\Delta G^\ddagger = 19.7$  kcal mol<sup>-1</sup>) when following an associative mechanism.

Having characterized all principal steps thus far, the precise knowledge of other steps that may lead to unwanted products is also of interest for the future development of improved catalysts. To this end, we have examined a diverging route that starts from **M2** involving  $\beta$ -hydride elimination. The most accessible pathway traverses a four-membered square-pyramidal TS structure, featuring cis disposed olefin and hydride units, which decays via smooth skeletal rearrangements into trigonal-bipyramidal Ir-cycloenammonium-hydrido compound **M5a** (Scheme 2).<sup>34</sup> Compared to the rival pathway, namely stepwise **M2a**  $\rightarrow$  **M3a**  $\rightarrow$  **M4b** Ir–C bond cleavage, the **M2c**  $\rightarrow$  **M5a**  $\beta$ -hydride elimination is predicted to be distinctly more demanding kinetically and is therefore not accessible.<sup>40</sup> These findings

may serve in rationalizing why the formation of pyrrolidines other than **6a** is not observed when using [Ir(COD)Cl]<sub>2</sub> as a precatalyst.

**Hydroamination via N–H Bond Activation.** An alternative hydroamination pathway involving N–H bond activation (Scheme 1, right) features the following elementary steps: (1) oxidative addition of the amine N–H linkage to the Ir<sup>I</sup> center; (2) insertion of the olefin unit into either Ir–N or Ir–H bonds of the resulting Ir<sup>III</sup>-amido-hydrido complex; (3) generation of the cycloamine by either C–H or C–N reductive elimination; and (4) liberation of the cycloamine by new substrate to regenerate **M1**. The condensed Gibbs free-energy profile, considering only the most accessible pathways for relevant steps, is displayed in Figure 8.

Commencing from the active compound **M1b**, oxidative addition of the amine N–H bond at the low-valent, coordinatively unsaturated Ir<sup>I</sup> center initially gives rise to the five-coordinate Ir<sup>III</sup>- $\eta^1$ -amidoalkene-hydrido compound **M6a**. The positional isomer participating along the most accessible pathway is depicted in Figure 8.<sup>34</sup> The square-planar structure of precursor **M1b** remains virtually undisturbed in the TS structure, which in turn decays into square-pyramidal **M6a**, featuring hydride in an axial position. Given the rather electron-deficient nature of the Ir<sup>I</sup> center in **M1b**, it comes as no surprise that this oxidative addition step imposes an almost insurmountable barrier of 38.2 kcal mol<sup>-1</sup> and is furthermore seen to be strongly endergonic ( $\Delta G = 25.7$  kcal mol<sup>-1</sup>), thereby rendering oxidative addition challenging on both kinetic and thermodynamic grounds in the present system. The uncoordinated C=C bond of the  $\eta^1$ (N)-amidoalkene-Ir unit in **M6a** can approach the metal center at its remaining coordination site, thereby giving rise to the six-coordinate Ir<sup>III</sup>- $\eta^2$ -amidoalkene-hydrido intermediate **M6'**. However, this supposedly facile conversion<sup>36</sup> comes at some thermodynamic cost, as **M6'** is less stable than **M6**. The several possible isomers of **M6'**, two of which are shown in Figure 8, are likely to interconvert readily.<sup>41</sup>

Two distinct paths for Ir-amidoalkene (**M6'**)  $\rightarrow$  Ir-cycloamine (**M4b**) transformation are conceivable, involving: (1) olefin insertion into the Ir<sup>III</sup>–N bond of **M6'** to afford Ir<sup>III</sup>-azacycle-hydrido intermediate **M7** with subsequent C–H reductive elimination; or (2) insertion of the double bond into the Ir<sup>III</sup>–H linkage of **M6'** and ensuing C–N reductive elimination under ring closure. The latter path is found to be more demanding energetically and well separated from the former and remains therefore virtually closed throughout the process.<sup>34</sup> DFT unveils that the dominant path toward pyrrolidine formation within this mechanistic manifold entails ring closure by insertion of the double bond into the Ir–N bond of **M6'**, followed by reductive C–H elimination from **M7**. Notably, this pathway is consistent with reports from Milstein,<sup>17a</sup> Togni<sup>17b</sup> and Hartwig<sup>18</sup> involving catalysts featuring a more electron-rich (bisphosphine)Ir fragment, which are known to proceed via activation of the N–H amine bond, and for which the barrier to N–H bond activation is presumably lower than in **M1b**.

Ring closure in **M6'** through double bond insertion into the Ir<sup>III</sup>–N bond has a modest barrier of 10.7 kcal mol<sup>-1</sup> and is strongly exergonic. The pathway that involves the thermodynamically favorable **M6'c**, where H and Cl occupy trans positions, is seen to be most accessible on both thermodynamic and kinetic grounds. Notably, the directly formed Ir<sup>III</sup>-azacycle-

(39) We have not determined the barrier for skeletal (polytopal) rearrangement between different forms of **M3**, but such processes are known to be facile.

(40) DFT predicts a kinetic gap of 11.9 kcal mol<sup>-1</sup> ( $\Delta\Delta G^\ddagger$ ) between stepwise protonolysis of the Ir–C bond and  $\beta$ -hydride elimination commencing from **M2**, in favor of the former, which leads us to confidently conclude that  $\beta$ -hydride elimination is not traversable.

(41) Note that the barriers for mutual interconversion via Berry rotation are generally considered to be low.

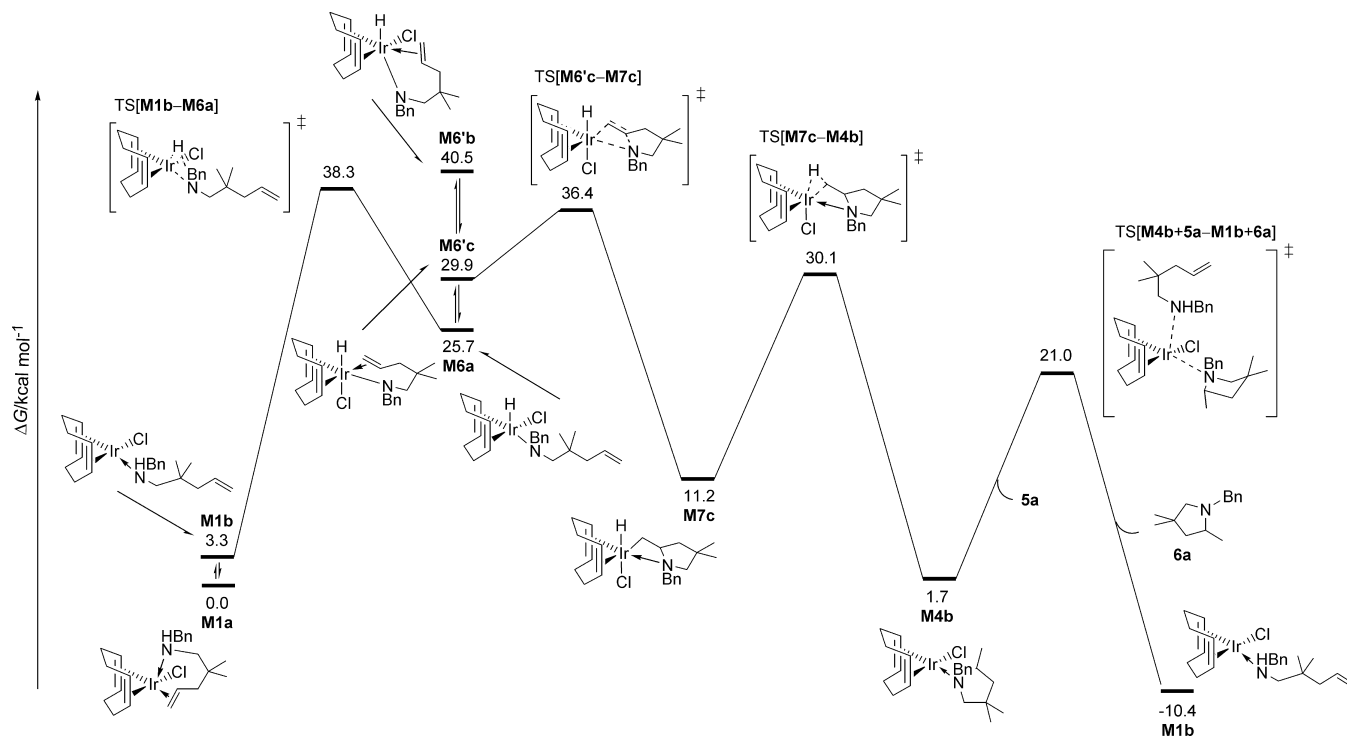


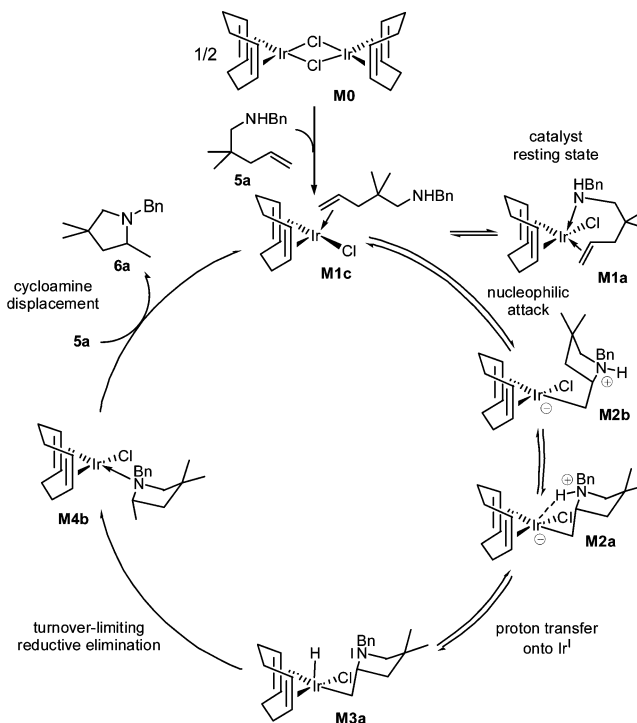
**Figure 8.** Free energy profile for the N–H bond activation route of intramolecular hydroamination of **5a** by [Ir(COD)Cl]<sub>2</sub> (**M0**). Only the most accessible pathway for all principal steps is shown, while alternative, but less favorable pathways are omitted for the sake of clarity.

hydrido species **M7c** must not undergo skeletal rearrangements prior to C–H reductive elimination. The lowest-energy pathway commencing from **M7c** has a barrier of 18.5 kcal mol<sup>−1</sup> to afford the Ir<sup>I</sup>–pyrrolidine compound **M4b**, which is downhill by another 9.5 kcal mol<sup>−1</sup>. Regeneration of **M1b** via associative displacement of pyrrolidine by substrate from **M4b** is almost identical energetically to the trajectory analyzed above that leads to **M1c**.

Hence, if the amine N–H bond were successfully to add to the Ir<sup>I</sup> center (as in (bisphosphine)Ir species<sup>16–18</sup>), subsequent conversion of the amidoalkene unit into pyrrolidine via **M6'c** → **M7c** → **M4b** would be kinetically viable and strongly downhill. As revealed from Figure 8 the first oxidative addition has the highest barrier and thus discriminates whether the N–H bond activation route can be traversed. The assessed unfavorable profile, featuring an almost insurmountable barrier of 38.3 kcal mol<sup>−1</sup> and being strongly uphill, is not compatible with the smooth hydroamination reported herein, and mitigates against N–H bond activation as being operative. This leads us to conclude that the route via initial amine activation (Scheme 1, right) is not accessible for the catalytically competent compound **M1** that features a rather electron-poor Ir<sup>I</sup> center, and instead the route via olefin activation (Scheme 1, left) prevails.

**Mechanistic Conclusions.** Our collective experimental and computational results lead us to the following mechanistic conclusions (Scheme 3). (1) Electrophilic activation of the C=C linkage by a relatively electron-poor Ir<sup>I</sup> center toward nucleophilic attack from the amine unit emerges as the operative mechanism for the [Ir(COD)Cl]<sub>2</sub>-catalyzed cyclohydroamination of unactivated aminoalkenes. (2) The [Ir(COD)Cl(substrate)] complex **M1** is the catalytically competent compound. (3) The most stable form of [Ir(COD)Cl(substrate)] is **M1a**, which features a chelating aminoalkene; **M1a** is the most abundant intermediate and therefore likely represents the catalyst resting state. Although **M1a** is a dormant species, it is easily converted into **M1c**, featuring η<sup>1</sup>-olefin–Ir ligation, to start the productive

**Scheme 3.** Proposed Mechanism for the [Ir(COD)Cl]<sub>2</sub>-Mediated Intramolecular Hydroamination of Aminoalkenes



catalytic cycle. (4) Ring closure via nucleophilic attack of the amine unit at the olefin functionality that is activated by coordination to the Ir center has a moderate barrier and is reversible. (5) Stepwise transfer of the proton from the ammonium unit in **M2a** onto the Ir center with subsequent C–H reductive elimination is the dominant pathway for cleavage of the Ir–C bond in the zwitterionic intermediate. The proton transfer step is kinetically viable and leads to the weakly



stabilized, transient five-coordinate Ir<sup>III</sup>-hydrido intermediate **M3a**, which thereafter undergoes reductive elimination by traversing a highly ordered six-coordinate TS structure. (6) The total activation energy for reductive elimination<sup>42a</sup> is highest among all relevant steps and as such this step must thus be considered as being turnover limiting. (7) Ensuing liberation of the cycloamine by incoming substrate is viable when following an associative pathway and regenerates the catalytically active **M1c** in an exergonic, hence irreversible step. In the context of this mechanistic scenario, the catalyst inhibition observed empirically for **1a**, **2a**, and DBU may be attributable in part to the action of these species as Brønsted bases toward the ammonium unit in **M2**. Alternatively, coordination of DBU to Ir could prevent substrate association in a manner that cannot be achieved by the weaker pyrrolidine base **2a**,<sup>42b</sup> thereby giving rise to a negligible population of the active compound **M1**. While the proposed olefin activation mechanism outlined in Scheme 3 is unprecedented for Ir-catalyzed alkene hydroamination,<sup>16–18</sup> comprehensive synthetic and mechanistic studies by Cochran and Michael<sup>8a</sup> support the operation of a related olefin activation pathway in the cyclohydroamination of unactivated alkenes bearing tethered amide/carbamate fragments mediated by cationic (PNP)Pd complexes. In keeping with our observations detailed herein, these workers noted a strong inverse dependence of the reaction rate on substrate concentration arising due to the reversible deprotonation of a [(PNP)Pd(alkylammonium)]<sup>2+</sup> intermediate by substrate, as well as rate-limiting Pd–C bond cleavage (protonolysis) involving this intermediate.<sup>8a</sup>

The assessed energy profile (Figure 7) is consonant with our observed empirical data. Turnover-limiting reductive elimination is consistent with the located highly organized TS structure and rationalizes the negative activation entropy measured. The lack of spectroscopic evidence for the putative Ir<sup>III</sup>-hydrido species **M3a** is understandable on the basis of its identification as a metastable intermediate, and rate-limiting reductive elimination from this intermediate is in keeping with the measured primary H/D KIE. Productive  $\beta$ -hydrogen elimination, as a potentially competitive event to productive hydroamination, proved not to be viable on the basis of computational data, thereby supporting the clean and efficient catalysis observed for several substrates. Finally, the assessed total barrier<sup>42a</sup> of 24.6 kcal mol<sup>–1</sup> for turnover-limiting reductive elimination agrees remarkably well with Eyring data for the cyclization of **1a** to **2a** (*vide supra*).<sup>42c</sup>

## Summary and Conclusions

We have identified [Ir(COD)Cl]<sub>2</sub> as a highly effective precatalyst for the intramolecular addition of primary as well as secondary alkyl- or arylamines to tethered unactivated olefins at relatively low catalyst loading. With the exception of the hydroamination of primary aminoalkenes, for which HNET<sub>3</sub>Cl was required as a cocatalyst, no coligands or additives were required in order to promote the hydroamination of these challenging substrates. In the quest to develop mechanistic insight into these intramolecular hydroamination reactions catalyzed by [Ir(COD)Cl]<sub>2</sub>, a comprehensive experimental and

computational investigation was conducted; notably, this represents the first such combined mechanistic study of the late metal-mediated cyclohydroamination of unactivated alkenes with secondary alkyl- and arylamines to appear in the literature. Collectively, the results of these studies reveal that these intramolecular hydroamination reactions commence from [Ir<sup>I</sup>-(COD)Cl(substrate)] as the catalytically competent compound and proceed via initial electrophilic activation of the olefin unit by a relatively electron-poor metal center, in a manner that has previously not been documented for Ir-catalyzed alkene hydroamination. An alternative mechanism involving activation of the amine functionality, which is firmly established for electron-rich Ir complexes, has proven inaccessible for the catalyst system under investigation herein. The operative mechanistic scenario involves: (1) smooth, reversible ring closure via nucleophilic attack of the amine on the metal coordinated, thus activated C=C bond; (2) stepwise cleavage of the Ir–C bond in the zwitterionic intermediate via proton transfer from the ammonium unit to Ir, with subsequent turnover-limiting C–H reductive elimination; and (3) associative displacement of the cycloamine by new substrate, thereby regenerating the active catalyst species. Turnover-limiting reductive elimination to involve a metastable, highly reactive Ir<sup>III</sup>-hydride intermediate and traversing a highly ordered TS structure is consistent with the measured primary H/D KIE and the observed negative activation entropy. DFT predicts an effective barrier for intramolecular hydroamination of a prototypical secondary alkylaminoalkene that is in remarkable agreement with observed activation parameters. Given the small number of late metal catalysts that have proven capable of promoting the intramolecular addition of primary and/or secondary alkyl- and arylamines to unactivated olefins, as well as the paucity of mechanistic data pertaining to these transformations, the catalytic and mechanistic findings reported herein represent an important contribution toward the development of increasingly effective late metal catalysts for use in mediating cyclohydroamination reactions.

## Experimental Section

**General Considerations.** All manipulations were conducted in the absence of oxygen and water under an atmosphere of dinitrogen, either by use of standard Schlenk methods or within an mBraun glovebox apparatus, utilizing glassware that was oven-dried (130 °C) and evacuated while hot prior to use. 1,4-Dioxane (Aldrich) was dried over Na/benzophenone followed by distillation under an atmosphere of dinitrogen. Toluene was deoxygenated by sparging with dinitrogen followed by passage through a double column solvent purification system purchased from mBraun Inc. 1,2-Dimethoxyethane and 1,2-dichloroethane were deoxygenated by sparging with dinitrogen gas followed by storage over activated 4 Å molecular sieves for 48 h prior to use. Chloroform-*d*<sub>1</sub> (Cambridge Isotopes) was used as received. All solvents used within the glovebox were stored over activated 4 Å molecular sieves. With the exception of [Ir(COD)<sub>2</sub>]<sup>+</sup>BF<sub>4</sub><sup>–</sup> and [Ir(MeCN)<sub>2</sub>(COD)]<sup>+</sup>BF<sub>4</sub><sup>–</sup>,<sup>43</sup> as well as 2-(di-*tert*-butylphosphino)-*N,N*-dimethylaniline<sup>44</sup> and [Pd(cinnamyl)Cl]<sub>2</sub>,<sup>45</sup> all of which were prepared using literature procedures, all other Rh and Ir complexes were purchased from Strem Chemicals and were evacuated under reduced pressure for 24 h prior to use. LiB(C<sub>6</sub>F<sub>5</sub>)<sub>4</sub>·2.5OEt<sub>2</sub> (Boulder Scientific), LiOTf (Strem), and AgBF<sub>4</sub> (Strem) were evacuated under reduced pressure

(42) (a) The absolute TOF-determining barrier is given relative to the catalyst resting state **M1a**. (b) DFT predicts that DBU binds more strongly in [Ir(COD)Cl(amine)] compounds than **1a** does in **M1a** by 12.0 kcal mol<sup>–1</sup>. On the other hand, the aminoalkene **1a** displaces pyrrolidine **2a** from **M4b** in a kinetically viable, downhill step (see Figure 7). (c) Cyclohydroamination of **1a** to **2a** has an observed turnover-limiting barrier of 27.7 kcal mol<sup>–1</sup> ( $\Delta G^\ddagger$ , 298 K).

(43) Green, M.; Kuc, T. A.; Taylor, S. H. *Chem. Commun.* **1970**, 1553.

(44) Lundgren, R. J.; Stradiotto, M. *Chem.—Eur. J.* **2008**, *14*, 10388.

(45) Auburn, P. R.; Mackenzie, P. B.; Bosnich, B. *J. Am. Chem. Soc.* **1985**, *107*, 2033.

for 24 h prior to use. 2,2-Diphenylpent-4-en-1-amine,<sup>11a</sup> (1-allylcyclohexyl)methanamine,<sup>11a</sup> 2,2-diphenylhex-5-en-1-amine,<sup>12</sup> 4-methyl-2,2-diphenylpent-4-en-1-amine,<sup>11a</sup> *N*-benzyl-2,2-diphenylpent-4-en-1-amine,<sup>6a</sup> methyl 4-[(2,2-diphenylpent-4-enylamino)methyl]benzoate,<sup>11a</sup> *N*-(4-methoxybenzyl)-2,2-diphenylpent-4-en-1-amine,<sup>6a</sup> *N*-(cyclohexylmethyl)-2,2-diphenylpent-4-en-1-amine,<sup>12</sup> (1-allylcyclohexyl)-*N*-benzylmethanamine,<sup>11a</sup> *N*-benzyl-2,2-dimethylpent-4-en-1-amine,<sup>11a</sup> 2-phenyl-2-(2-propenyl)-1-amino-4-pentene,<sup>46</sup> *N*-benzyl-2-isopropylpent-4-en-1-amine,<sup>11a</sup> *N*-benzyl-2,2-diphenylhex-5-en-1-amine,<sup>12</sup> *N*-benzyl-4-methyl-2,2-diphenylpent-4-en-1-amine,<sup>47</sup> benzyl[1-(2-methylallyl)-cyclohexylmethyl]amine,<sup>11a</sup> (*E*)-*N*-benzyl-2,2-diphenylhex-4-en-1-amine and (*Z*)-*N*-benzyl-2,2-diphenylhex-4-en-1-amine,<sup>14</sup> *tert*-butyl-2,2-diphenylpent-4-enylcarbamate,<sup>8c</sup> *N*-phenyl-2,2-diphenylpent-4-en-1-amine,<sup>14</sup> *N*-(4-methylphenyl)-2,2-diphenylpent-4-en-1-amine,<sup>14</sup> *N*-(4-methoxyphenyl)-2,2-diphenylpent-4-en-1-amine,<sup>14</sup> *N*-(4-fluorophenyl)-2,2-diphenylpent-4-en-1-amine,<sup>14</sup> (1-allylcyclohexyl)-*N*-phenylmethanamine,<sup>48</sup> *N*-phenyl-2,2-diphenylhex-5-en-1-amine,<sup>48</sup> and *N*-phenyl-4-methyl-2,2-diphenylpent-4-en-1-amine,<sup>48</sup> were synthesized according to literature procedures. All other reagents were used as received. <sup>1</sup>H and <sup>13</sup>C NMR characterization data were collected at 300 K on a Bruker AV-500 spectrometer operating at 500.1 and 125.8 MHz (respectively) with chemical shifts reported in parts per million downfield of SiMe<sub>4</sub>. Conductivity measurements were carried out on a VWR SympHony pH/Conductivity meter employing a VWR SympHony 4 carbon probe conductivity cell with 0.55 cm<sup>-1</sup> cell constant; calibrations were made with 1.12 microSeimens and 100,039 microSeimens Traceable conductivity solutions. The curve fittings were carried out using the program SigmaPlot for Windows v. 10.0 (Systat Software, San Jose, CA).

**Representative Procedure for the Intramolecular Hydroamination of Unactivated Alkenes by Secondary Alkylamines (Table 2).** To a screw-capped vial containing **1a** (82 mg, 0.25 mmol) and a stir-bar was added 0.125 mL of a stock solution of [Ir(COD)Cl]<sub>2</sub> (2.6 mg, 0.0039 mmol) in 1.548 mL of 1,4-dioxane ([Ir] = 0.005 mM) and 0.375 mL of dioxane (total reaction volume = 0.5 mL). The vial was sealed under N<sub>2</sub> with a cap containing a PTFE septum and, once all the material had dissolved, was removed from the glovebox and was placed in a temperature-controlled aluminum heating block set at 110 °C. After 3 h of magnetic stirring the vial was removed from the temperature-controlled aluminum heating block, cooled to ambient temperature, diluted with CH<sub>2</sub>Cl<sub>2</sub> (2 mL), and was washed with brine (2 × 5 mL). The organic extracts were combined, dried over Na<sub>2</sub>SO<sub>4</sub>, and concentrated. The resulting residue was purified by flash column chromatography on silica gel (hexanes/EtOAc = 20:1) to yield **2a** as a white solid (72 mg, 0.22 mmol, 88%) that afforded analytical data in agreement with data reported in the literature.<sup>11a</sup>

**Representative Procedure for the Intramolecular Hydroamination of Unactivated Alkenes by Arylamines (Table 3).** To a screw-capped vial containing *N*-phenyl-2,2-diphenylpent-4-en-1-amine (78 mg, 0.25 mmol) and a stir-bar was added 0.5 mL of a stock solution of [Ir(COD)Cl]<sub>2</sub> (5.7 mg, 0.0085 mmol) in 1.357 mL of 1,4-dioxane ([Ir] = 0.0125 mM). The vial was sealed under N<sub>2</sub> with a cap containing a PTFE septum and, once all the material had dissolved, was removed from the glovebox and was placed in a temperature-controlled aluminum heating block set at 110 °C. After 7 h of magnetic stirring the vial was removed from the temperature-controlled aluminum heating block, cooled to ambient temperature, diluted with CH<sub>2</sub>Cl<sub>2</sub> (2 mL), and was washed with brine (2 × 5 mL). The organic extracts were combined, dried over Na<sub>2</sub>SO<sub>4</sub>, and concentrated. The resulting residue was purified by

flash column chromatography on silica gel (hexanes/EtOAc = 10:1) to afford 1-phenyl-2-methyl-4,4-diphenylpyrrolidine as a colorless oil that solidified to a white solid upon standing (74 mg, 0.22 mmol, 95%), and for which obtained characterization data agreed with data reported in the literature.<sup>14</sup>

#### Representative Procedure for the Intramolecular Hydroamination of Unactivated Alkenes by Primary Amines (Table 4).

To a screw-capped vial containing 2,2-diphenylpent-4-en-1-amine (59 mg, 0.25 mmol), triethylammonium chloride (1.7 mg, 0.0125 mmol) and a stir-bar was added 0.5 mL of a stock solution of [Ir(COD)Cl]<sub>2</sub> (21 mg, 0.031 mmol) in 2.548 mL of 1,4-dioxane ([Ir] = 0.025 mM). The vial was sealed under N<sub>2</sub> with a cap containing a PTFE septum and, once all the material had dissolved, was removed from the glovebox and was placed in a temperature-controlled aluminum heating block set at 110 °C. After 24 h of magnetic stirring the vial was removed from the temperature-controlled aluminum heating block, cooled to ambient temperature, diluted with CH<sub>2</sub>Cl<sub>2</sub> (2 mL), and was washed with brine (2 × 5 mL). The organic extracts were combined, dried over Na<sub>2</sub>SO<sub>4</sub>, and concentrated. The resulting residue was purified by flash column chromatography on silica gel (CH<sub>2</sub>Cl<sub>2</sub>/MeOH = 10:1) to yield 2-methyl-4,4-diphenylpyrrolidine as a pale-yellow oil (53 mg, 0.22 mmol, 89%) that afforded analytical data in agreement with data reported in the literature.<sup>12</sup>

**Computational Section.** All calculations based on Kohn–Sham density functional theory (DFT)<sup>49</sup> were performed by means of the program package TURBOMOLE<sup>50</sup> using the almost nonempirical meta-GGA Tao–Perdew–Staroverov–Scuseria (TPSS) functional<sup>51</sup> within the RI-J integral approximation<sup>52</sup> in conjunction with flexible basis sets of triple- $\zeta$  quality. For iridium we used the Stuttgart–Dresden scalar-relativistic effective core potential (SDD, 60 core electrons)<sup>53</sup> in combination with the (8s7p6d1f)/[6s5p3d1f] (def2-TZVP) valence basis set.<sup>54</sup> All remaining elements were represented by Ahlrich’s valence triple- $\zeta$  TZVP basis set<sup>55</sup> with polarization functions on all atoms. The good to excellent performance of the TPSS functional for a wide range of applications, with transition-metal complexes in particular, has been demonstrated previously.<sup>56</sup> The energy landscape of the entire cyclohydroamination course was assessed for the secondary alkylamine **5a** together with [Ir(COD)Cl]<sub>2</sub> **M0** as precatalyst (entry 2–7 in Table 2). No structural simplification of any of the involved key species was imposed. The DFT calculations have simulated the authentic reaction conditions by treating bulk effects of the 1,4-dioxane solvent by a consistent polarizable continuum model.<sup>57</sup> All the stationary points were fully

(46) Majumder, S.; Odom, A. L. *Organometallics* **2008**, *27*, 1174.

(47) Dochnahl, M.; Pissarek, J.-W.; Blechert, S.; Löhnitz, K.; Roesky, P. W. *Chem. Commun.* **2006**, 3405.

(48) Lundgren, R. J.; Sappong-Kumankumah, A.; Stradiotto, M. *Chem.–Eur. J.*

(49) Parr, R. G.; Yang, W. *Density-Functional Theory of Atoms and Molecules*; Oxford University Press: Oxford, 1989.

(50) (a) Ahlrichs, R.; Bär, M.; Häser, M.; Horn, H.; Kölmel, C. *Chem. Phys. Lett.* **1989**, *162*, 165. (b) Treutler, O.; Ahlrichs, R. *J. Chem. Phys.* **1995**, *102*, 346. (c) Ahlrichs, R.; Furche, F.; Hättig, C.; Klopper, W.; Sierka, M.; Weigend, F. *TURBOMOLE, version 6.0*; University of Karlsruhe: Karlsruhe, Germany, 2009; <http://www.turbomole.com>. (51) (a) Dirac, P. A. M. *Proc. R. Soc. London* **1929**, *A123*, 714. (b) Slater, J. C. *Phys. Rev.* **1951**, *81*, 385. (c) Perdew, J. P.; Wang, Y. *Phys. Rev.* **1992**, *B45*, 13244. (d) Tao, J.; Perdew, J. P.; Staroverov, V. N.; Scuseria, G. E. *Phys. Rev. Lett.* **2003**, *91*, 146401. (e) Perdew, J. P.; Tao, J.; Staroverov, V. N.; Scuseria, G. E. *J. Chem. Phys.* **2004**, *120*, 6898.

(52) (a) Vahtras, O.; Almlöf, J.; Feyereisen, M. W. *Chem. Phys. Lett.* **1993**, *213*, 514. (b) Eichkorn, K.; Treutler, O.; Öhm, H.; Häser, M.; Ahlrichs, R. *Chem. Phys. Lett.* **1995**, *242*, 652.

(53) Andrae, D.; Häussermann, U.; Dolg, M.; Stoll, H.; Preuss, H. *Theor. Chim. Acta* **1990**, *77*, 123.

(54) (a) Weigend, F.; Ahlrichs, R. *Phys. Chem. Chem. Phys.* **2005**, *7*, 3297. (b) Weigend, F. *Phys. Chem. Chem. Phys.* **2006**, *8*, 1057.

(55) (a) Schäfer, A.; Huber, C.; Ahlrichs, R. *J. Chem. Phys.* **1994**, *100*, 5829. (b) Eichkorn, K.; Weigend, F.; Treutler, O.; Ahlrichs, R. *Theor. Chem. Acc.* **1997**, *97*, 119.

(56) (a) Staroverov, V. N.; Scuseria, G. E.; Tao, J.; Perdew, J. P. *J. Chem. Phys.* **2003**, *119*, 12129. (b) Zao, Y.; Truhlar, D. G. *J. Chem. Theory Comput.* **2005**, *1*, 415. (c) Furche, F.; Perdew, J. P. *J. Chem. Phys.* **2006**, *124*, 044103.

(57) Klamt, A.; Schüürmann, G. *J. Chem. Soc., Perkin Trans 2* **1993**, 799.

located with inclusion of solvation. Analytical frequency calculations were performed to confirm the nature of all optimized key structures and to determine thermodynamic parameters (298 K, 1 atm) under the rigid-rotor and harmonic approximations. The mechanistic conclusions drawn in this study were based on the Gibbs free-energy profile of the entire catalytic cycle assessed at the TPSS(COSMO)/SDD+TZVP level of approximation for experimental condensed phase conditions. Further details together with a description of the employed computational methodology are given in the Supporting Information. Calculated structures were visualized by employing the StrukEd program,<sup>58</sup> which was also used for the preparation of 3D molecule drawings.

**Acknowledgment.** We thank the Natural Sciences and Engineering Research Council of Canada (including a Discovery Grant

for M. S. and a Canada Graduate Scholarship for K.D.H.) and Dalhousie University (M.S. and K.D.H.) for their generous support of this work. We also thank Dr. Michael Lumsden (NMR3, Dalhousie) for assistance in the acquisition of NMR data, and Prof. Heather Andreas (Dalhousie) for assistance in conducting solution conductivity measurements.

**Supporting Information Available:** Complete experimental procedures and characterization data, including tabulated experimental results and supporting NMR data, computational details, detailed computational characterization of relevant elementary steps, and Cartesian coordinates of all calculated species. This material is available free of charge via the Internet at <http://pubs.acs.org>.

JA908316N

---

(58) For further details, see <http://www.struked.de>.